The Plant Cell, Vol. 25: 324–341, January 2013, www.plantcell.org

Endodermal ABA Signaling Promotes Lateral Root Quiescence during Salt Stress in *Arabidopsis* Seedlings[C][W]

Lina Duan,[a,b,c] Daniela Dietrich,[d] Chong Han Ng,[b] Penny Mei Yeen Chan,[b,c] Rishikesh Bhalerao,[e] Malcolm J. Bennett,[d] and José R. Dinneny[a,b,c,1]

[a] Carnegie Institution for Science, Department of Plant Biology, Stanford, California 94305
[b] Temasek Lifesciences Laboratory, National University of Singapore, 117604, Singapore
[c] Department of Biological Sciences, National University of Singapore, 117604, Singapore
[d] Plant Sciences Division, School of Biosciences, University of Nottingham, Loughborough LE12 5RD, United Kingdom
[e] Umeå Plant Science Centre, Department of Forest Genetics and Plant Physiology, Swedish University of Agricultural Sciences, S-901 83 Umea, Sweden

The endodermal tissue layer is found in the roots of vascular plants and functions as a semipermeable barrier, regulating the transport of solutes from the soil into the vascular stream. As a gateway for solutes, the endodermis may also serve as an important site for sensing and responding to useful or toxic substances in the environment. Here, we show that high salinity, an environmental stress widely impacting agricultural land, regulates growth of the seedling root system through a signaling network operating primarily in the endodermis. We report that salt stress induces an extended quiescent phase in postemergence lateral roots (LRs) whereby the rate of growth is suppressed for several days before recovery begins. Quiescence is correlated with sustained abscisic acid (ABA) response in LRs and is dependent upon genes necessary for ABA biosynthesis, signaling, and transcriptional regulation. We use a tissue-specific strategy to identify the key cell layers where ABA signaling acts to regulate growth. In the endodermis, misexpression of the ABA insensitive1-1 mutant protein, which dominantly inhibits ABA signaling, leads to a substantial recovery in LR growth under salt stress conditions. Gibberellic acid signaling, which antagonizes the ABA pathway, also acts primarily in the endodermis, and we define the crosstalk between these two hormones. Our results identify the endodermis as a gateway with an ABA-dependent guard, which prevents root growth into saline environments.

INTRODUCTION

Root system architecture is a complex emergent property of the root that arises due to the growth attributes of the primary root (PR), individual lateral roots (LRs), and adventitious roots. In many Eudicot species, the PR is specified during embryogenesis and establishes the majority of the root system through the production of LRs along its length. In *Arabidopsis thaliana*, the patterning of LR founder cell populations occurs at regular temporal intervals and leads to the specification of founder cell populations that later develop into LR primordia (De Smet et al., 2007; Moreno-Risueno et al., 2010). Subsequent to primordia formation, the process of LR emergence requires that the primordium communicate with the outer tissue layers of the root to coordinate changes in tissue integrity with the destructive process of outgrowth (Swarup et al., 2008). Much attention has focused on these initial stages of LR development, and auxin signaling and transport are critical components at every stage of this process (Benková et al., 2003; De Smet et al., 2007; Dubrovsky et al., 2008; Laskowski et al., 2008; Moreno-Risueno et al., 2010; Overvoorde et al., 2010).

Postemergence LR development is tightly controlled by environmental stimuli, such as nutrient and water availability (López-Bucio et al., 2003; Malamy, 2005). Nitrate, for example, can inhibit LR elongation through competition with auxin transportation and by affecting mitotic activity (Little et al., 2005; Okushima et al., 2011). Localized sources of iron, by contrast, promote LR growth by triggering auxin accumulation in root apices through the regulated expression of the auxin influx carrier *AUXIN 1* (*AUX1*) (Giehl et al., 2012). Intrinsic differences in the environmental response programs of PRs and LRs have also been observed. Phosphate promotes PR growth and inhibits LR growth (Zhang and Forde, 1998; Linkohr et al., 2002), though the mechanistic basis for these differences is unknown. The water stress–associated hormone abscisic acid (ABA) is a known inhibitor of LR development and has been shown to act at the postemergence stage (Signora et al., 2001; De Smet et al., 2003). ABA has a much stronger effect on LR than PR growth, suggesting that differences in environmental responsiveness between these two root types may be due to divergent hormone signaling networks.

Recent work using cell type–specific profiling methods has demonstrated that tissue identity is critical for providing a context

[1] Address correspondence to dinneny@stanford.edu.
The author responsible for distribution of materials integral to the findings presented in this article in accordance with the policy described in the Instructions for Authors (www.plantcell.org) is: José R. Dinneny (dinneny@stanford.edu).
[C] Some figures in this article are displayed in color online but in black and white in the print edition.
[W] Online version contains Web-only data.
www.plantcell.org/cgi/doi/10.1105/tpc.112.107227

in which environmental responses are interpreted at the cellular level (Dinneny, 2010; Wee and Dinneny, 2010). Changes in salinity, nutrient content, pH, and oxygen concentration all elicit a large number of transcriptional and posttranscriptional changes that substantially differ between each cell type (Dinneny et al., 2008; Gifford et al., 2008; Mustroph et al., 2009; Iyer-Pascuzzi et al., 2011). These data have led to a sophisticated understanding of the biological pathways targeted by environmental regulation, but it is still unclear what the tissue-specific regulatory mechanisms that control these changes are.

Plant hormones are important secondary signaling molecules that mediate responses to many environmental stimuli, and recent work has shown that several of these hormones promote growth primarily by acting in specific tissue layers. Brassinosteroid signaling acts in the epidermis to promote shoot growth (Savaldi-Goldstein et al., 2007) and regulate root meristem size (González-García et al., 2011; Hacham et al., 2011), while gibberellic acid (GA) signaling leads to the degradation of DELLA proteins, which negatively regulate growth primarily in the endodermal tissue layer (Ubeda-Tomás et al., 2008, 2009). These results suggest a possible mechanism by which environmental stimuli elicit localized transcriptional changes through the action of hormones that trigger tissue-specific signaling cascades. Hormones associated with stress responses also regulate growth of the plant (Spollen et al., 2000; Sharp and LeNoble, 2002; Achard et al., 2006), but it is not known whether the growth-suppressing activities of these hormones also act in specific cell layers.

Here, we dissect the tissue-specific function of ABA signaling in regulating root growth to reveal the mechanism by which salt controls root system architecture in the seedling. High salinity is an important and prevalent agricultural contaminant that affects yield (Flowers et al., 1997), and previous studies have shown that elevated salt levels can inhibit both PR and LR growth (Burssens et al., 2000; He et al., 2005). We reveal that PR and postemergence-stage LR growth show divergent temporal dynamics during salt stress, which is due to LR-specific ABA signaling. We identify the endodermis as the key tissue layer required for ABA-mediated growth repression of the LR during salt stress and dissect points of crosstalk with the GA pathway in this process. These data provide insight into a previously uncharacterized function of the endodermis as a sentinel cell layer, which guards against growth into saline environments.

RESULTS

The Growth of Primary and LRs Is Differentially Affected by Salt Stress

Root system architecture is determined by three fundamental parameters: (1) the number of LR branch points specified along the PR, (2) the initiation and emergence rates for these LR primordia, and (3) the growth rate of each root type, the PR, and postemergence LRs. Adventitious roots, which develop at the root-hypocotyl junction, are considered a special type of LR and are not studied here. To quantify the effect of salt stress on these three parameters, *Arabidopsis* seedlings were grown on standard media for 6 d postgermination (dpg) and then transferred to standard conditions or media supplemented with sodium chloride (NaCl) and grown for an additional 4 d post-transfer (dpt). This treatment established two regions along the PR: region A (for above transfer point), in which the PR had grown before the transfer to salt conditions; and region B (for below transfer point), in which the PR had grown after the transfer (Figure 1A). Based on recent work, the patterning of LRs is determined close to the root tip, and initiation of LR primordia from founder cells occurs later in development (De Smet et al., 2007; Moreno-Risueno et al., 2010; Overvoorde et al., 2010). Thus, LR patterning in region A is expected to have occurred before treatment of roots with high salinity. Consistent with this hypothesis, we found that high salinity had little effect on the total number of LRs initiated in region A (Figure 1B) (Malamy and Benfey, 1997). Furthermore, we did not observe any strong effects on the distribution of developmental stages for preemergent LR primordia (Figure 1B). In region B, the number of emerged LRs was clearly suppressed and the total number of LRs was lower, suggesting that LR initiation or founder cell specification is inhibited by salt treatment (Figure 1C). Further investigation of the mechanisms affecting the patterning of LRs in region B is the subject of another study and is not discussed further here.

While the total number of LRs initiated and the developmental progression of preemergent LR primordia was not affected in region A, measurement of the total or average postemergence LR length revealed that salt had a strong inhibitory effect on growth at this stage of development (Figure 1D; see Supplemental Figure 1A online). Interestingly, PR growth was much less sensitive to salt treatment compared with LR growth (49.6% compared with 84.3% reduction, respectively, at 100 mM NaCl) (Figure 1D). These differences were observed in multiple accessions of *Arabidopsis*, despite differences in overall salt sensitivity (see Supplemental Figures 1B and 1C online).

Developmental Age Affects the Sensitivity of the LR, but Not the PR, to Salt Stress

Our observed differences in the response of LRs and PRs to salt stress could have two potential causes, which are not mutually exclusive. First, in our experiments, we measured the response of PRs 6 dpg, but LR growth was measured after emergence from the PR. Thus, differences in salt response could be a consequence of the developmental age of the specific root type. A second possibility is that LRs and PRs differ in their salt responses due to an inherent difference in the signaling properties of the organ. Testing the first possibility is complicated by the fact that PRs and LRs are defined by fundamentally different times of origin (embryonic versus postembryonic) and positions of formation (de novo formation versus endogenous development within the PR). Thus, there is no stage of PR development that is equivalent to a postemergent LR. Nevertheless, we can ask the question of whether the salt response profile changes with developmental age for the PR or LR.

We transferred seedlings grown for between 2 to 8 dpg to media supplemented with 100 mM NaCl and found that the sensitivity of the PR did not significantly differ between these

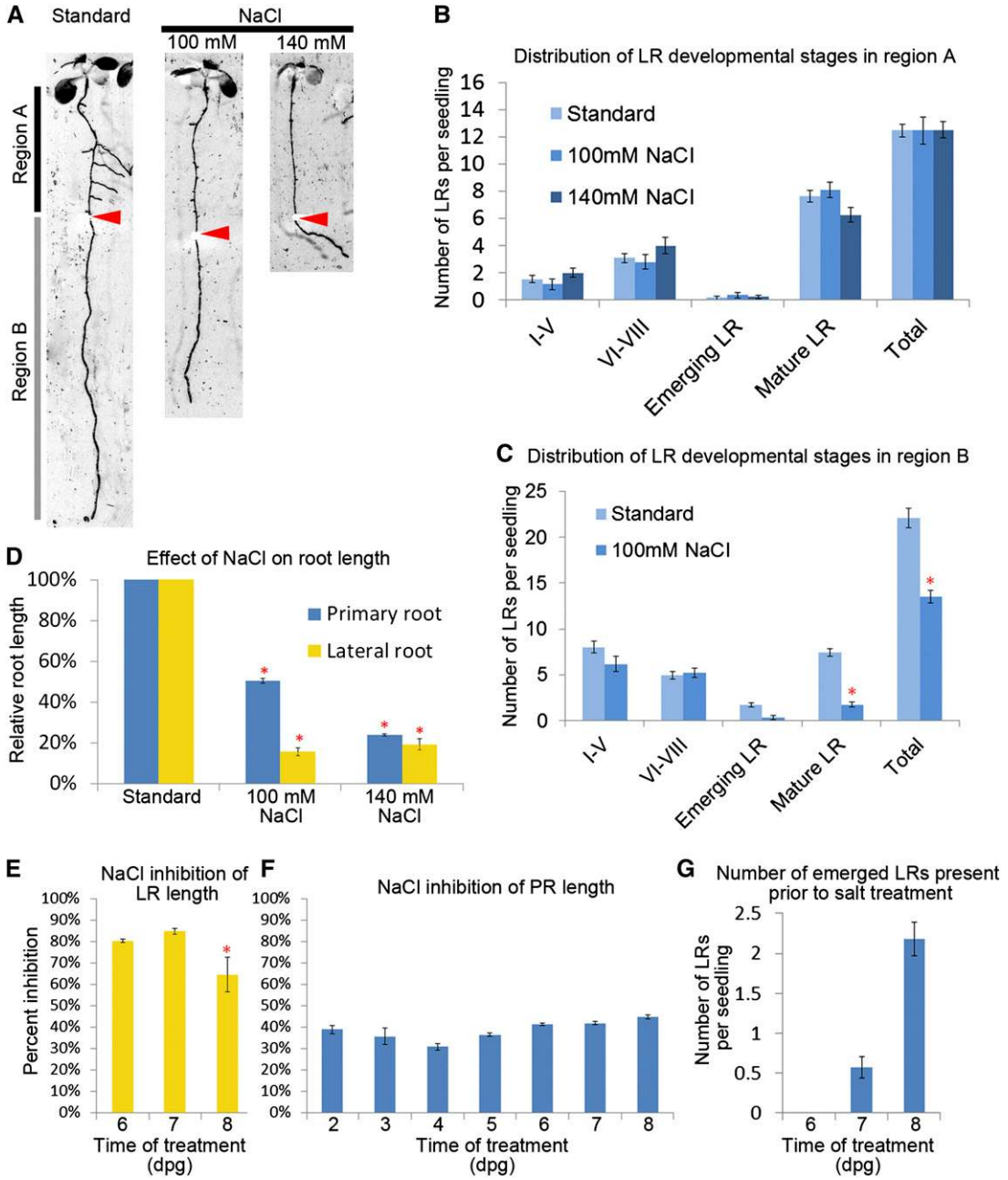

Figure 1. The Growth of PRs and LRs Is Differentially Affected by Salt Stress.

(A) Morphology of the Col-0 root system grown on standard media for 6 dpg then transferred to standard, 100 mM NaCl, or 140 mM NaCl media conditions for 4 d. Arrowheads mark the position of the root tip at the time of transfer from standard to treatment conditions.
(B) and **(C)** Quantitation of preemergent and late stages of LR development in root region A **(B)** and region B **(C)** after transfer to standard or salt stress conditions ($n > 10$ seedlings).
(D) Average PR and LR length for seedlings transferred to 100 or 140 mM NaCl. Measurements are expressed as a percentage of the length under standard conditions ($n > 20$ seedlings).
(E) and **(F)** Suppression of LR **(E)** and PR **(F)** growth under 100 mM NaCl conditions measured as a percentage of reduction relative to standard conditions. Seedlings were transferred to salt at different days postgermination (dpg) and grown for 4 dpt ($n > 8$ seedlings).
(G) Number of emerged LRs formed in 6, 7, or 8 dpg seedlings before transfer ($n > 30$ seedlings).
Error bars indicate SE. Asterisks mark significant changes in salt response based on a Student's *t* test, P value < 0.05.
[See online article for color version of this figure.]

seedlings (Figure 1F). Measurement of growth rates in roots that had just emerged from the seed coat also did not reveal any obvious hypersensitivity to salt stress at this earliest developmental stage (see Supplemental Figures 1E and 1F online). Thus, PRs consistently show relative resistance to salt treatment throughout initial seedling development. LRs, by contrast, showed a decrease in sensitivity to salt when seedlings were transferred at 8 dpg compared with 6 or 7 dpg (Figure 1E). This difference is correlated with the prevalence of postemergence stage LRs at the time of transfer (Figure 1G) and indicates that only newly emerged LRs are hypersensitive to salt treatment.

Postemergence Growth Quiescence Is Induced in LRs by Salt Stress

To understand how salt stress severely inhibits LR growth and why a specific LR developmental stage may be required, live imaging was used to monitor the temporal dynamics of growth regulation. Growth rates of postemergence LRs were quantified for 7 dpt on standard or saline media. Interestingly, growth was not stably suppressed throughout the salt response, but instead, LRs were maintained in a quiescent stage for several days (Figures 2A and 2B; see Supplemental Movie 1 online). Similar quiescent LRs were observed under standard conditions, however, much less frequently. After several days of quiescence, LRs resumed growth at rates similar to roots grown under standard conditions (Figure 2B). This response dynamic differed substantially for the PR, which showed an immediate recovery of growth after being transferred to salt stress conditions (see Supplemental Figure 1D online). We examined the expression of the cell cycle marker *CYCB1;1*:*GUS* (for β-glucuronidase) and found that expression was greatly reduced in quiescent-stage LR primordia (Figures 2C and 2D) (de Almeida Engler et al., 1999). No changes in the structure of the stem cell niche or radial organization, which could affect growth rates, were observed in quiescent stage LRs (see Supplemental Figure 2 online). Together, these results indicate that salt induces a period of quiescence in LRs, which may be, in part, a consequence of suppressed cell cycle activity.

ABA Signaling Is Necessary for LR Growth Suppression during Salt Stress

ABA acts as an important secondary signaling molecule during abiotic stress (Sharp and LeNoble, 2002; Zhu, 2002; De Smet et al., 2003; Hubbard et al., 2010). Under high salinity, the production of ABA is induced and its signaling pathways are necessary for salt tolerance (Achard et al., 2006). We first treated roots with varying concentrations of ABA to determine if this hormone treatment had an effect similar to high salinity. As previously shown (De Smet et al., 2003), ABA treatment affected LR growth more severely than PR growth (63.0% compared with 15.6% reduction, respectively, after treatment with 1 μM ABA) (Figure 3A). To determine whether LRs are generally more sensitive to the effects of growth-suppressing hormones, we treated seedlings with 1-aminocyclopropane-1-carboxylic acid (ACC), a biosynthetic precursor to ethylene, which is also induced under salt stress (Achard et al., 2006). Interestingly, ACC treatment caused the opposite trend in growth, having a much stronger effect on PR than LR growth (72.3% compared with 46.8% reduction, respectively, after treatment with 1 μM ACC) (Figure 3B). Other ecotypes also showed similar responses to NaCl, ABA, and ACC (see Supplemental Figure 3 online). Together, these results indicate that LRs and PRs are distinguished based on both their hormone and stress response profiles. The similarity in the response of the root system to NaCl and ABA suggests that this hormone may be most critical for eliciting the suppression of growth in LRs.

To test whether endogenous hormone signaling is responsible for root system architecture changes in the seedling during salt stress, we measured the effect of salt on average LR length for various mutants disrupted in the ABA pathway. This analysis identified mutations affecting ABA biosynthesis (*ABA DEFICIENT2 alleles* [aba2-1 or aba2-sail]), signal transduction (*aba insensitive1-1* [*abi1-1*]), and transcriptional regulation (*aba insensitive4-1 fusca3-3*) that mediate salt-dependent LR growth suppression (Figure 3C; see Supplemental Figure 4A online). Importantly, none of these mutations significantly affected PR growth under these conditions, which suggests that the ABA response may be restricted to the LR during salt stress (see Supplemental Figure 4B online).

We also examined the role of ethylene signaling in LR growth suppression by salt stress. The *ethylene insensitive 2-44* (*ein2-44*) mutant, which strongly disrupts ethylene signaling (Ghassemian et al., 2000), showed moderately higher sensitivity to salt stress, indicating that ethylene signaling may promote LR growth under these conditions (see Supplemental Figures 4C and 4D online). The *like aux1 3* (*lax3*) mutant, which affects auxin transport and is necessary for LR emergence (Swarup et al., 2008), did not significantly impact the salt response of postemergent LR.

The Endodermis Is the Target Cell Layer for ABA-Dependent Salt Stress Regulation of LR Growth

Several plant hormones have been shown to regulate growth through tissue-specific signaling (Swarup et al., 2005; Savaldi-Goldstein et al., 2007; Ubeda-Tomás et al., 2008, 2009; González-García et al., 2011; Hacham et al., 2011). To determine if ABA operates by a similar principle, we used the GAL4-VP16/UAS enhancer trap system (Kiegle et al., 2000; Ubeda-Tomás et al., 2008) to drive tissue-specific expression of *abi1-1*, which dominantly suppresses ABA signaling. *ABI1* encodes a PP2C-type protein phosphatase and ABA coreceptor, which dephosphorylates SnRK-type kinases to inhibit ABA-dependent signal transduction (Meyer et al., 1994; Fujii et al., 2009; Ma et al., 2009; Park et al., 2009). The *abi1-1* mutation renders the protein constitutively active, and overexpression of the mutant coding sequence can be used to dominantly suppress ABA signaling (Leung et al., 1997). We verified that the enhancer-trap lines used in our study drive strong expression in the various cell layers of PRs and postemergence LRs using the associated *UAS*:*erGFP* reporter (Figures 4A to 4C; see Supplemental Figure 5 online).

We first determined whether tissue-specific expression of *abi1-1* could induce resistance to exogenous application of 10 μM ABA, which affects PR and LR growth to a similar extent as

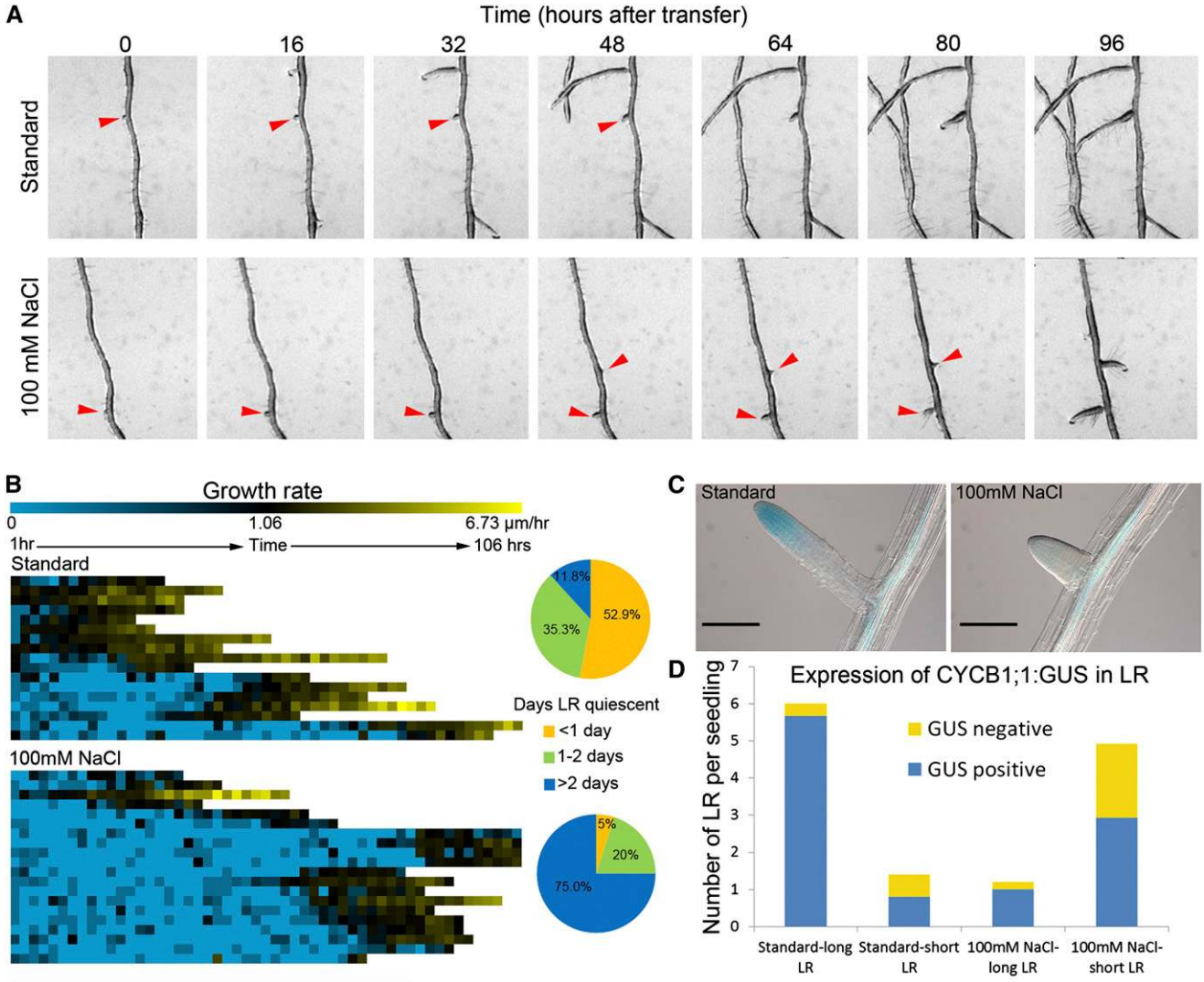

Figure 2. A Prolonged Quiescent Phase Is Induced during Salt Stress in Postemergent LRs.

(A) Time-lapse images of 6 dpg Col-0 seedlings after transfer to standard conditions (top panels) or 100 mM NaCl conditions (bottom panels). Red arrowheads mark quiescent LRs.

(B) Heat map showing the growth profiles of individual LRs quantified from time-lapse imaging data. Each pixel in the heat map represents the total growth over 2 h. Data quantified from 10 to 12 seedlings transferred to standard (n = 17 LRs) or salt stress (n = 20 LRs) conditions and imaged for 7 dpt. Pie charts to the right of the heat maps quantify the proportion of LRs that are quiescent for different lengths of time. Salt stress causes a dramatic increase in the number of roots showing quiescent growth for more than 2 d.

(C) Staining pattern of the *CYCB1;1*:*GUS* reporter in postemergent LRs 3 dpt to standard conditions (left panel) or to 100 mM NaCl conditions (right panel). Bars = 100 µm.

(D) Quantification of *CYCB1;1*:*GUS* activity at different stages of postemergent LR development under standard or salt stress conditions (n = 15 individual seedlings). LRs were categorized as long or short based on the presence of a clear elongation and maturation zone. More LRs are shorter under salt stress conditions and these roots often lack GUS reporter expression.

100 mM NaCl. F1 seedlings generated by a cross between a *UAS*:*abi1-1* transgenic plant and the various enhancer trap lines conferred reduced sensitivity of LR growth to ABA treatment when expression was driven in the ground tissue (*J0571*), endodermis and pericycle (*Q2500*), or stele (*Q0990*) (Figures 4D and 4F). This pattern of activity partially overlaps with the cell layers observed to be important for ABA signaling in the PR, where enhancer traps driving *abi1-1* expression in the epidermis and cortex (*J2812*), ground tissue layers (*J0571*), and endodermis and pericycle (*Q2500*) had a significant effect, but stele expression (*Q0990*) did not (Figures 4D and 4G). These results indicate that *abi1-1*–dependent ABA signaling acts to regulate growth in a spatially restricted fashion and that the ground tissue layers are common sites for such regulation in the PR and LR.

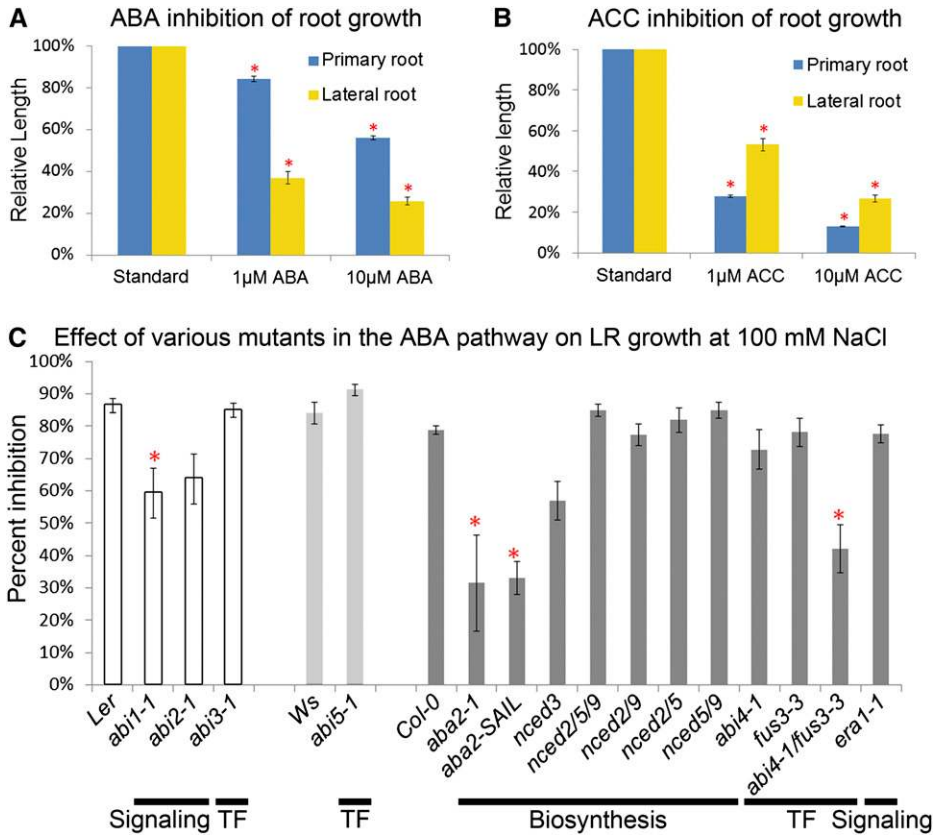

Figure 3. LR Growth Is Hypersensitive to ABA Treatment and Mutants Disrupting the ABA Signaling Pathway Affect Salt-Mediated Suppression of LR Growth.

(A) and **(B)** Relative PR and LR length quantified 4 dpt to media supplemented with 1 or 10 μM ABA **(A)** or 1 or 10 μM **(B)** ACC ($n > 20$ seedlings).
(C) Mutants disrupting ABA biosynthesis, signal transduction, or transcriptional regulation were surveyed for defects in the response to 100 mM NaCl. The average length of all LRs per seedling was measured and the percentage of difference between salt stress and standard conditions was calculated and shown in the graph. Mutations in the *Ler* background are shown as white bars, Ws background as light-gray bars, and Col-0 background as dark-gray bars ($n > 15$ seedlings). TF, transcription factor.
All seedlings grown for 6 dpg and average LR length per seedling measured 4 dpt. Error bars indicate SE. Asterisks mark significant changes in salt response based on a Student's *t* test, P value < 0.05, with Bonferroni correction.
[See online article for color version of this figure.]

We next asked whether salt stress–dependent ABA signaling acts through similar tissue layers as exogenous ABA treatment. Here, *abi1-1* was most effective at rescuing LR growth when expressed in the endodermal and pericycle tissue layers of LRs (*Q2500*) or in the ground tissue as a whole (*J0571*) and less so when expressed in the epidermis and cortex (*J2812*) (Figures 4E and 4F). Use of a pericycle-specific enhancer trap (*J0121*) to drive *abi1-1* expression had a very mild effect on LR length during ABA or salt treatment (see Supplemental Figure 6 online), which suggested that endodermal expression of *abi1-1* in the *Q2500* line is the primary cause of the reduced sensitivity to ABA or salt. Expression of *abi1-1* in the various tissue layers had little effect on PR growth under salt stress conditions (Figures 4E and 4G), consistent with the LR specificity of the ABA response we inferred from our genetic analysis. Our media contains 1% Suc, but we found that this did not significantly affect the ABA-dependent regulation of LR growth during salt stress treatment (see Supplemental Figure 7 online).

To confirm the function of ABA signaling in the ground tissue during salt stress, an endodermis-specific gene promoter, *ProSCARECROW* (*ProSCR*) (Figure 4H) (Di Laurenzio et al., 1996), and a cortex-specific promoter, *ProCORTEX* (*ProCOR*) (Lee et al., 2006), were used to drive the expression of an *abi1-1*:*RFP* (for red fluorescent protein) translational fusion. Two independent *ProSCR*:*abi1-1*:*RFP* transgenic lines showed rescue of LR growth under both ABA and salt treatment (see Supplemental Figure 8A online). Fluorescence imaging of these lines revealed weak but endodermal-specific localization (see Supplemental Figure 8C online). These results were further confirmed by transforming plants with a *ProSCR*:*abi1-1* transgene lacking any fluorescent tag (Figure 4I). The *ProCOR*:*abi1-1*:*RFP* lines also showed a rescue in LR growth with ABA or salt treatment (see Supplemental Figure 8B online). However, we found that the abi1-1:RFP fusion protein showed cortex and endodermal localization, suggesting that the promoter used to

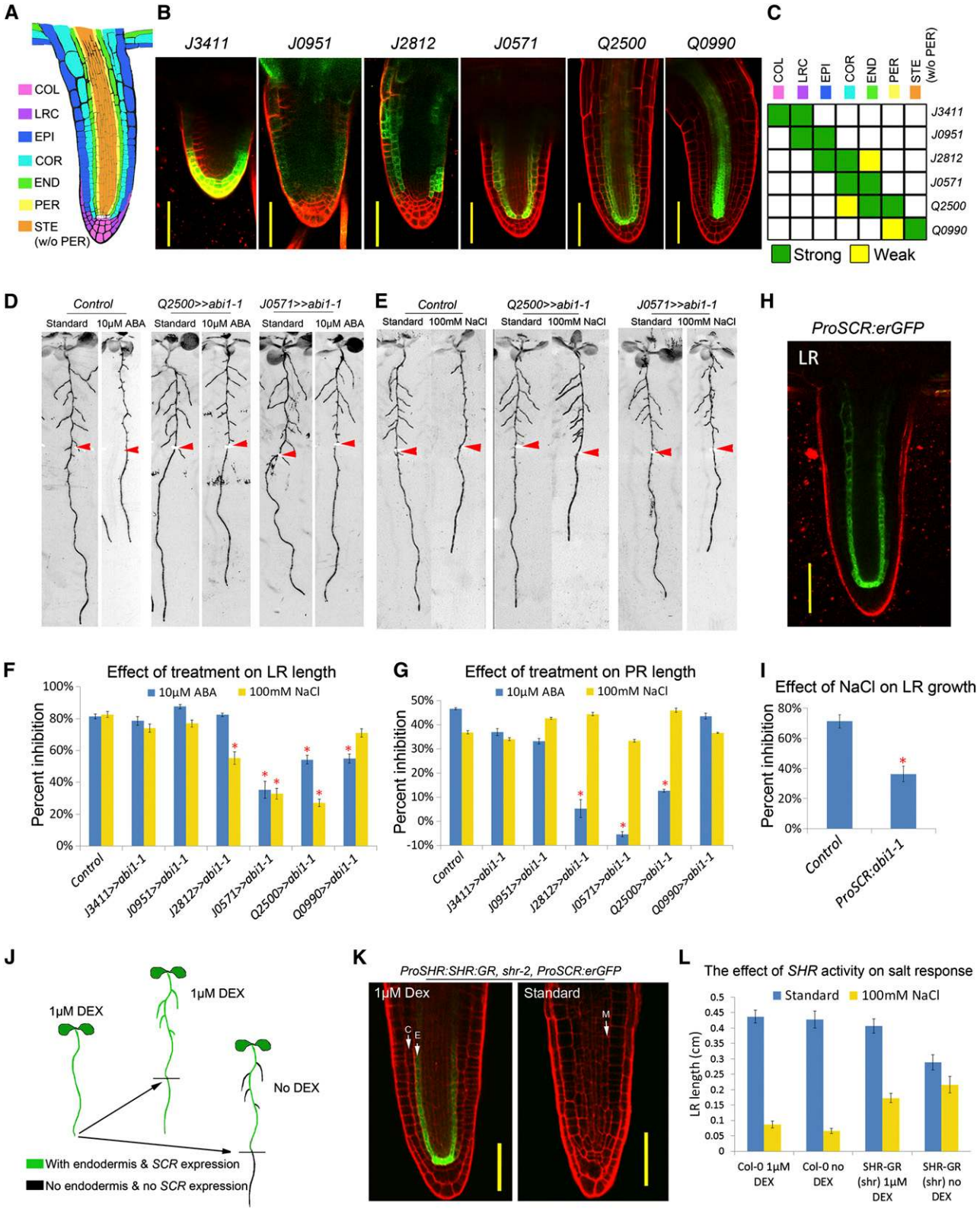

Figure 4. The Endodermis Is an Important Site for ABA Signaling and Growth Regulation during Salt Stress.

drive transgene expression may not have cortex-specific activity or that the abi1-1 protein has limited ability to move between tissue layers (see Supplemental Figure 8D online). Together, our data indicate that ABA signaling acts primarily in the endodermis to limit LR growth during salt stress conditions, although we cannot exclude the possibility that the cortex may also have some importance in this process. These data also show that the pattern of activity for the ABA pathway is environmentally dependent, with salt acting through a more restricted domain of the root than with exogenous ABA treatment.

Our results suggest a model in which the endodermis is the source of a growth-promoting activity in the LR that is suppressed by salt stress through the execution of an ABA-dependent response in this cell type. To explore this model further, we next asked how loss of the endodermis might affect the salt responsiveness of the LR. SHORTROOT (SHR) is a GRAS family transcription factor necessary to promote periclinal division of the cortex/endodermal stem cell and the subsequent specification of endodermal identity in one of the two daughter cells (Helariutta et al., 2000; Cui et al., 2007). The *shr* mutant lacks an endodermis in both PRs and LRs and affects the morphogenesis of LRs (Lucas et al., 2011). To avoid some of the nonspecific effects of the *shr* mutant, we used a dexamethasone (DEX)–inducible *SHRpro*:*SHR-GR*, *shr-2*, *ProSCR*:*erGFP* line, which is able to fully rescue the mutant phenotype (Levesque et al., 2006; Sozzani et al., 2010). The *ProSCR*:*erGFP* reporter is directly regulated by SHR and is a marker for endodermal identity. Seedlings were initially grown on media supplemented with 1 μM DEX for 6 dpg and then transferred to media with or without 100 mM NaCl and/or 1 μM DEX (Figure 4J). We analyzed the expression of the *SCR* reporter and observed that an endodermis only formed in LRs developing on DEX-supplemented media (Figure 4K). Interestingly, we observed that LRs lacking DEX treatment grew more slowly under standard conditions and showed little response to salt, whereas DEX-treated LRs responded more similarly to wild-type plants (Figure 4L). These data are consistent with our model and support the hypothesis that endodermal signaling in the LR itself is key to the regulation of postemergence growth.

Sustained ABA Signaling Is Associated with LR Quiescence during Salt Stress

To determine if the quiescence of LRs is correlated with the timing of ABA signaling, we examined the activity of an ABA-responsive reporter driven by the *RESPONSIVE TO ABA18* (*RAB18*) promoter, *ProRAB18*:*GFP* (Kim et al., 2011), in the root system after salt treatment. Under standard conditions, *ProRAB18*:*GFP* was expressed at very low levels in both the PR and LRs (Figures 5A, 5B, and 5D). During salt stress, *ProRAB18*:*GFP* was weakly expressed in the PR (Figure 5A). During LR development, reporter expression was also weak just after emergence but became highly induced ~2 d later (Figures 5A, 5C, and 5D). Reporter expression in postemergence LRs was maintained at very high levels for several days until the time at which growth resumed, when it decreased (Figures 5C and 5D). The substantially higher level of ABA signaling in the LR, compared with the PR, explains why the suppression of ABA signaling by our various perturbations had an LR-specific effect on growth. In response to ABA treatment, *ProRAB18*:*GFP* was also induced after LR emergence as it entered into a quiescent phase; however, expression was maintained for a longer time period (see Supplemental Figures 9B and 9C online). We analyzed the induction of ABA signaling in older root systems and found that LRs, which escaped growth suppression by salt stress, also lacked induction of the *ProRAB18*:*GFP* reporter,

Figure 4. (continued).

(A) A false-colored drawing of a LR illustrating the different cell types present. COL, columella root cap; COR, cortex; END, endodermis; EPI, epidermis; LRC, lateral root cap; PER, pericycle; STE, stele without pericycle.

(B) Confocal images of the various *GAL4-VP16*/*UAS* enhancer trap lines used in this study showing the activity of the associated *UAS*:*erGFP* reporter in postemergent LRs.

(C) Heat map summarizing the relative expression level of the various enhancer trap lines.

(D) and **(E)** Images of root systems for the control genotype, *Q2500>>abi1-1*, and *J0571>>abi1-1* transactivation lines 4 dpt to standard conditions, 10 μM ABA treatment **(D)**, or 100 mM NaCl conditions **(E)**. Red arrowheads mark the position of the root tip at the time of transfer.

(F) and **(G)** The average length of all LRs **(F)** or PRs **(G)** per seedling was measured and the percentage of difference between the treatment and standard conditions was calculated and shown in the graph. Growth suppression by 4 dpt to 100 mM NaCl conditions or 10 μM ABA conditions is shown ($n > 20$ seedlings).

(H) Confocal image of *ProSCR*:*erGFP* expression in a postemergent LR is localized to the endodermis.

(I) Percentage of difference in LR length of the *ProSCR*:*abi1-1* transgenic line 4 dpt to 100 mM NaCl conditions ($n > 18$ seedlings).

(J) Diagram illustrating our experimental design for studying the effects of genetically ablating the endodermal tissue layer specifically in LRs. The *ProSHR*:*SHR*:*GR*, *shr-2*, *ProSCR*:*erGFP* line was grown on media supplemented with 1 μM DEX for 6 dpg then transferred to media with or without DEX. In the diagram, green portions of the root have an endodermis and *ProSCR*:*erGFP* reporter activity.

(K) Confocal images of the *ProSHR*:*SHR*:*GR*, *shr-2*, *ProSCR*:*erGFP* line in LRs, which developed after transfer to media with (left panel) or without (right panel) DEX. With DEX treatment, GFP expression driven by the *ProSCR*:*erGFP* marks the endodermis, while only a mutant cell layer (M) exists without it. c, cortex; e, endodermis.

(L) Quantitation of LR length in Col-0 and the *ProSHR*:*SHR*:*GR*, *shr-2*, *ProSCR*:*erGFP* transgenic line 4 dpt to standard conditions or 100 mM NaCl-supplemented media with or without 1 μM DEX ($n > 17$ seedlings).

Error bars indicate SE. Red asterisks mark significant differences based on a two-way analysis of variance and Student's *t* test, P value < 0.05. Bars = 50 μm.

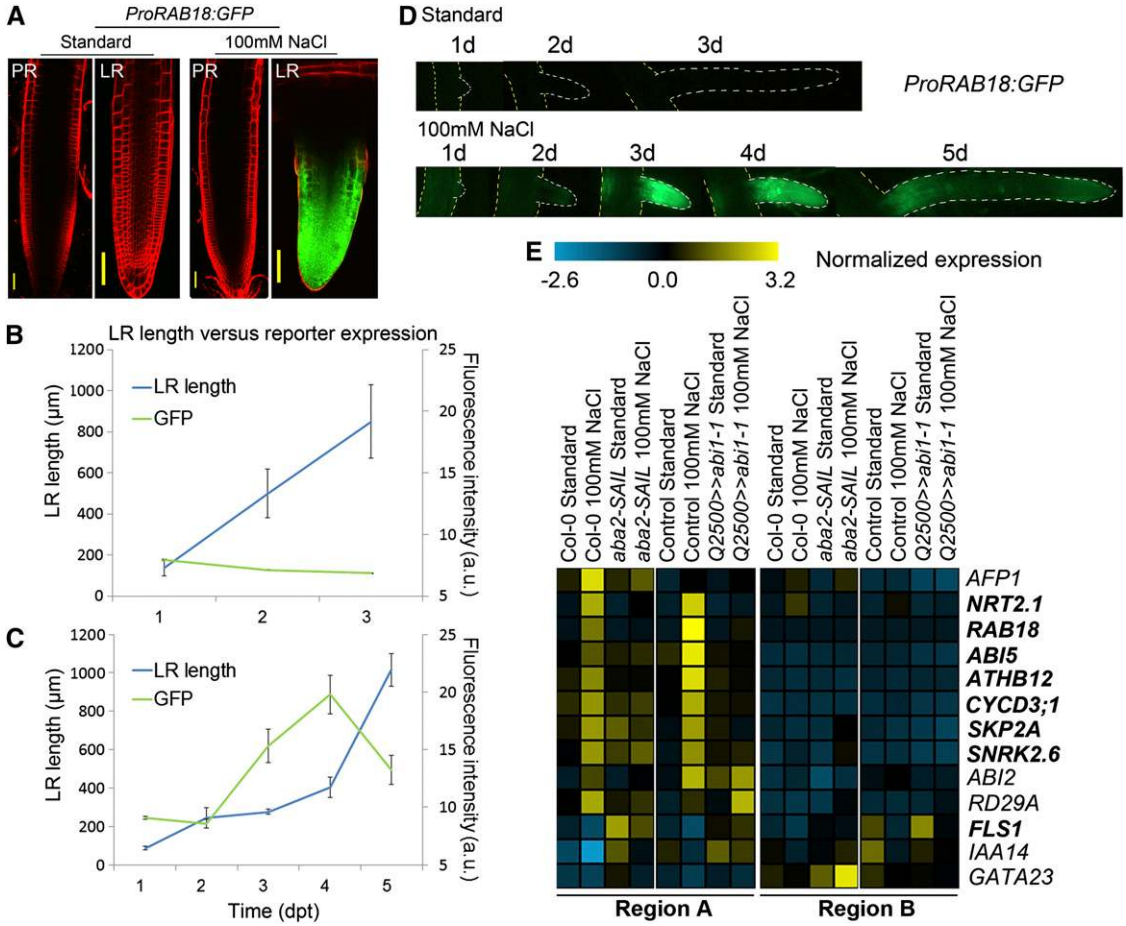

Figure 5. ABA Signaling Is Selectively Induced in LRs and Correlates with Growth Quiescence.

(A) Seedlings with the *ProRAB18*:*GFP* reporter were transferred to standard or 100 mM NaCl media and PRs or LRs imaged by confocal microscopy. Bars = 50 μm.

(B) and **(C)** Quantification of LR length and *ProRAB18*:*GFP* fluorescence intensity in seedlings transferred to standard conditions for 1 to 3 d post-transfer (dpt) **(B)** or 100 mM NaCl for 1 to 5 dpt **(C)** (n = 15 seedlings). Error bars indicate SE. a.u., arbitrary units.

(D) Time-lapse images of *ProRAB18:GFP* expression in LRs after transfer to standard or 100 mM NaCl conditions.

(E) Gene expression analysis of ABA-dependent salt responsive genes using high-throughput qRT-PCR. Expression was measured 3 dpt to standard or 100 mM NaCl media from root region A and region B, separately. Expression measured in Col-0, *aba2-SAIL*, enhancer trap control, and the *Q2500>>abi1-1* transactivation line. Heat map shows normalized gene expression values averaged from two biological replicates and three technical replicates. Gene expression profiles were organized by hierarchical clustering. Bold highlighted genes showed dependency on endodermal ABA signaling.

while LRs entering quiescence showed strong expression (see Supplemental Figure 9D online). Together, these data show that salt-induced growth quiescence is tightly correlated with the activation of ABA signaling.

To confirm and extend our results, we used high-throughput quantitative RT-PCR (qRT-PCR) to analyze salt-regulated changes in expression for a collection of ABA-responsive genes. Seedlings were grown on standard media for 6 dpg and then transferred to standard conditions or media supplemented with NaCl and grown for an additional 3 dpt. RNA was isolated from either region A or B of the root system from Columbia-0 (Col-0), *aba2-sail*, the *Q2500>>abi1-1* transactivation line, or the associated control. Known ABA-inducible genes (*RESPONSIVE TO DESICCATION 29A* [*RD29A*] and *ABI2*) and others showed strong transcriptional activation by salt stress predominantly in region A, which contains postemergent LRs, while expression was much reduced in region B (Figure 5E). Induction of *RAB18* expression by salt was alleviated in the *aba2-sail* mutant and also strongly reduced in the *Q2500>>abi1-1* transactivation line (Figure 5E). The tissue-specific expression pattern of the *ProRAB18*:*GFP* reporter is not informative since it uses a non-localized GFP reporter protein, which may translocate between cell layers. However, based on cell type–specific transcriptional profiling data (Winter et al., 2007; Dinneny et al., 2008), *RAB18* is most strongly activated in the endodermis and moderately induced in the cortex (see Supplemental Figure 9A online). However, an important caveat applies to the analysis of such data, since it was generated from PRs treated with 140 mM NaCl

(Dinneny et al., 2008). Analysis of other salt-responsive genes identified several that were also strongly dependent upon ABA signaling in the endodermis, including *HOMEOBOX12* (*HB12*), an ABA-induced gene necessary for growth suppression during water stress (Figure 5E) (Olsson et al., 2004; Son et al., 2010). These data show that ABA signaling is enriched in the region of the root-containing LRs and that endodermal ABA signaling is necessary for many of these responses.

Live-imaging analysis of the *Q2500>>abi1-1* transactivation line revealed that postemergent LRs showed an immediate activation of growth under salt conditions (Figure 6; see Supplemental Movie 2 online), which confirms that ABA signaling in this subdomain of the LR is critical for maintaining quiescence. Interestingly, LR growth was not sustained in *Q2500>>abi1-1*, and after a few days, growth became arrested and the roots senesced (Figures 6B and 6C; 66.7% of all LRs). In control plants, LR growth was sustainable after recovery from quiescence throughout the duration of the imaging session (Figure 6A).

Nutrients Enhance the ABA-Dependent Effect of NaCl on LR Growth

Differences in the response of PRs and LRs to changes in nutrient levels have previously been described, and responses to high levels of nitrate are known to be ABA dependent (Signora et al., 2001). Thus, we asked whether nutrient concentration in our media might also modulate the response to salt stress. In the PR, we found that increasing concentrations of Murashige and Skoog (MS) nutrient salts reduced the effect of NaCl on growth (see Supplemental Figure 10A online). This effect is consistent with previous studies showing that increasing levels of certain nutrients, such as potassium (Zhu et al., 1998), can provide protection against the ionic stress caused by sodium. Interestingly, we saw the opposite trend for LRs, which became more sensitive to NaCl as the concentration of MS nutrients increased (see Supplemental Figure 10B online). The suppression of LR growth at full-strength MS is strongly affected in the *Q2500>>abi1-1* transactivation line, but this transgene had little

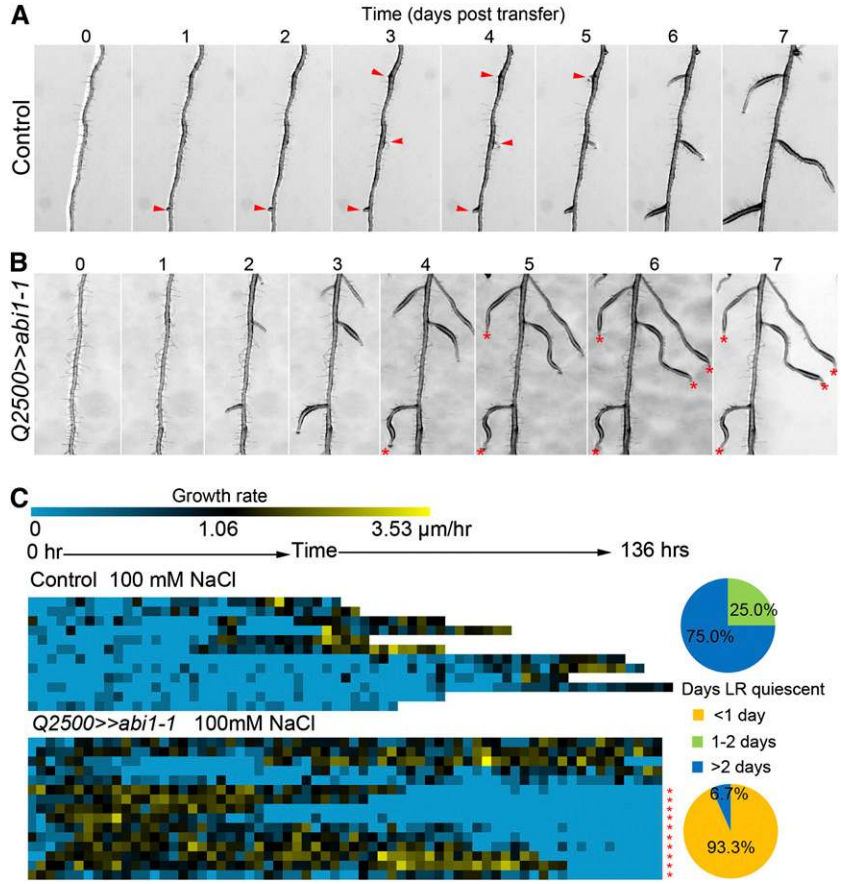

Figure 6. Suppression of Endodermal ABA Signaling Leads to a Loss of Salt-Induced Quiescence and Unsustainable Growth Recovery.

(A) and **(B)** Time-lapse images of enhancer trap control **(A)** or *Q2500>>abi1-1* transactivation seedlings **(B)** after transfer to 100 mM NaCl conditions. Red arrowheads mark quiescent LRs. Red asterisks mark LRs that showed unsustainable growth recovery.

(C) Heat map showing the growth profiles of individual LRs quantified from time-lapse imaging data. Each pixel in the heat map represents the total growth over 2 h. Data quantified from enhancer trap control seedlings (n = 12 LRs) or *Q2500>>abi1-1* transactivation seedlings (n = 15 LRs) transferred to 100 mM NaCl conditions and imaged for 7 d. Pie charts to the right of the heat maps quantify the proportion of LRs that are quiescent for different lengths of time. Red asterisks mark LRs that show unsustainable growth recovery, 10 out of 15.

impact in media containing quarter-strength MS. These data provide evidence that nutrients can alter the decision-making process of the root, as it relates to salt response, and that these effects are dependent on root type– and tissue-specific ABA signaling.

GA Signaling Acts in Parallel and Antagonistically with ABA in LRs

Our data show that postemergence LRs undergo a period of quiescence during salt stress, which is induced by ABA. Another phase of plant development characterized by an ABA-dependent period of growth arrest is seed dormancy (Finkelstein et al., 2008). Here, GA acts antagonistically to promote germination. To test whether GA may also suppress LR quiescence, we treated roots with varying concentrations of GA during salt stress. With GA treatment, the suppression of LR growth by salt was significantly reduced (Figure 7A). Time-lapse imaging of LRs under GA-supplemented salt stress conditions showed that the timing of growth recovery was hastened by hormone treatment (Figure 7B). PR growth was less sensitive to GA treatment, again highlighting important differences in hormone signaling between the two root types (see Supplemental Figure 11A online).

To understand what function endogenous GA levels might have in regulating growth during salt stress, we studied the effects of the GA biosynthesis inhibitor paclobutrazol (PAC). Under standard conditions, PAC treatment suppressed LR growth, indicating that GA biosynthesis is important under this condition (Figure 7C). The *abi1-1* mutation partially suppressed this effect, indicating that PAC treatment affects LR growth, in part, by elevating ABA signaling. PAC was not able to fully suppress the *abi1-1* phenotype under salt stress conditions, which suggests that *abi1-1* also acts to regulate growth independent of changes

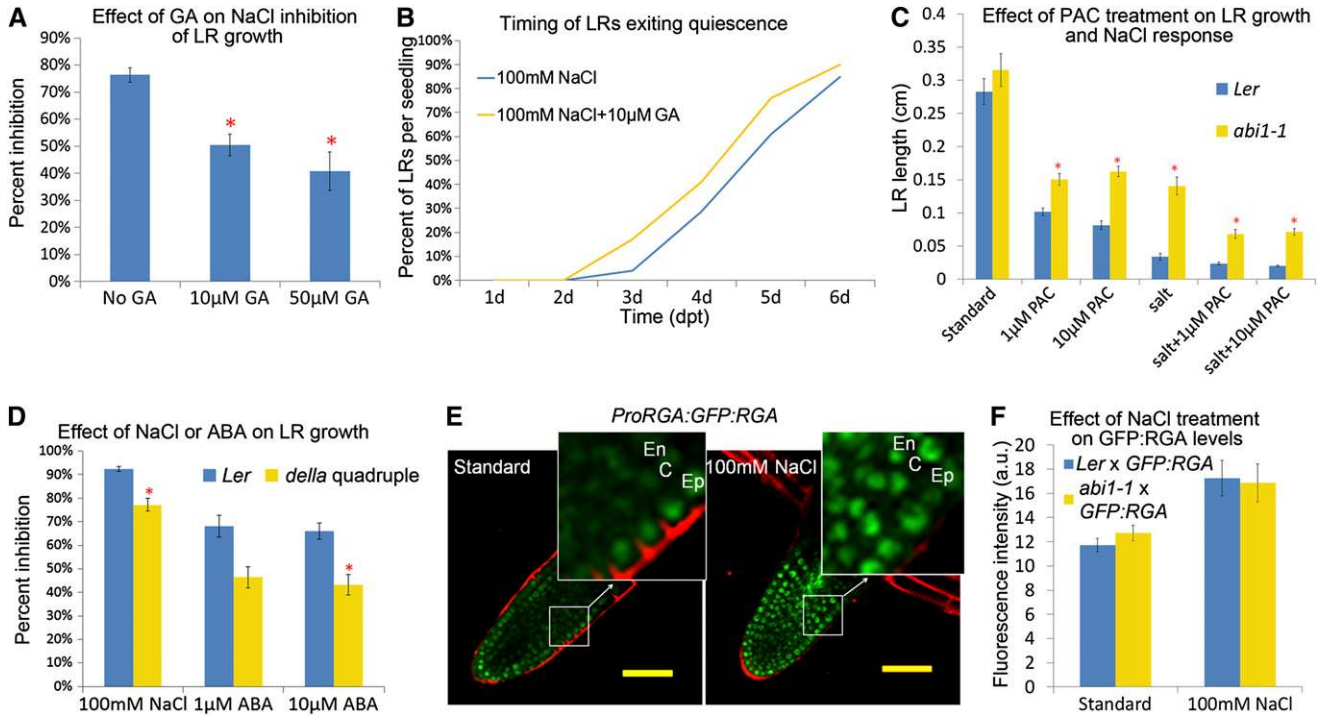

Figure 7. Integration of GA and ABA Signaling Pathways during Salt Stress.

(A) Percentage of difference in average LR length per seedling quantified 4 dpt to media containing 100 mM NaCl compared with control conditions. Media was supplemented with 0, 10, or 50 μM GA ($n > 20$ seedlings). Ecotype used here is Col-0.

(B) Percentage of LRs (*ProRAB18*:*GFP*) that had exited quiescence after transfer to 100 mM NaCl with or without 10 μM GA. Emerged LRs were followed on six to 10 individual seedlings over 6 d. LRs that were shorter than 0.5 mm in length were categorized as quiescent.

(C) Average length of LRs per seedling for L*er* and *abi1-1* mutants measured 4 dpt to standard or 100 mM NaCl media supplemented with various concentrations of the GA biosynthesis inhibitor, PAC ($n > 17$ seedlings).

(D) Percentage of difference in the average LR length per seedling 4 dpt to media supplemented with 100 mM NaCl or two different concentrations of ABA. Genotype is L*er* or the *della* quadruple mutant ($n > 20$ individual seedlings).

(E) Confocal images of postemergence stage LRs grown under standard (left panel) or 100 mM NaCl (right panel) conditions and expressing the *ProRGA*:*GFP-RGA* reporter. Bars = 50 μm. En, endodermis; C, cortex; Ep, epidermis.

(F) Quantification of GFP fluorescence intensity in F1 hybrid plants generated by a cross between L*er* and *ProRGA*:*GFP:RGA* or *abi1-1* −/− and *ProRGA*:*GFP:RGA*. Seedlings grown for 3 dpt to standard or 100 mM NaCl conditions ($n > 8$ LRs). a.u., arbitrary units.

Error bars indicate SE. Red asterisks represent significant differences as determined by the Student's *t* test, P value < 0.05.

in GA biosynthesis (Figure 7C). Together, these data show that ABA and GA signaling act in opposing ways to regulate LR growth and that this regulation occurs through mutual antagonism as well as through independent pathways.

GA signal transduction leads to the degradation of the DELLA class of growth repressors (Achard et al., 2006; Harberd et al., 2009; Skirycz and Inzé, 2010). Consistently, the *della* quadruple mutant combination caused a partial rescue in LR growth under salt-stress conditions (Figure 7D). PR growth was also affected in this mutant, but less severely (see Supplemental Figure 11B online). Previous work has shown that ABA or salt treatment can stabilize DELLA proteins in PRs (Achard et al., 2006). The effect of salt stress on DELLA protein levels was examined in both LRs and PRs using the *REPRESSOR OF GA* (*RGA*) reporter, *ProRGA*:*GFP*:*RGA*. In salt-treated quiescence-stage LRs, we observed relatively high levels of GFP:RGA in all tissue layers, including the endodermis (Figure 7E), whereas PRs maintained much lower levels (see Supplemental Figure 11C online). Previous studies have identified the endodermis as the key site for DELLA-dependent growth regulation of the PR (Ubeda-Tomás et al., 2008, 2009). We observed that DELLA activity in the endodermis also suppressed the growth of LRs (see Supplemental Figure 12C online). We asked whether the increase in RGA protein levels is dependent upon ABA signaling by visualizing GFP:RGA fluorescence in an *abi1-1* mutant background. Interestingly, we did not see a change in fluorescence levels even though LR growth was clearly rescued (Figure 7E; see Supplemental Figures 12A and 12B online). These data suggest that ABA may partly act through non-DELLA-dependent mechanisms to inhibit LR growth. Consistent with this model, we found that the *della* quadruple mutant only showed a moderate reduction in ABA sensitivity (Figure 7D) and did not suppress ABA-dependent changes in gene expression during the salt stress response (see Supplemental Figure 12D online).

DISCUSSION

Our study reveals an important interplay between developmental and environmental pathways that ultimately transforms the root system architecture of the seedling to suit a new environmental condition. We show that LRs and PRs have intrinsically different response programs to salinity and the associated hormones elicited downstream with ABA being the critical effector of LR growth. The site of action for this hormone is primarily localized to the endodermis, thus highlighting how cell identity provides an important signaling context for salt stress responses. Finally, the ultimate outcome of the stress signaling network outlined here is to dynamically control the growth of LRs, which will cause a transformation in the emergent properties of the seedling root system due to changes in the ratio between LR and PR growth. We hypothesize that these differences are likely related to the unique functions of each root type in a typical Eudicot taproot system; the PR functions to extend the root system into deeper terrain, while LRs exploit the resources identified at specific depths. We speculate that LR-specific activation of ABA signaling will shift the balance of root growth toward soil exploration, away from resource acquisition.

The Root System Is Composed of Root Types with Distinct Salt Stress and Hormone Signaling Properties

The *Arabidopsis* root system is composed of primary, lateral, and adventitious roots. LRs are differentiated from the PR due to their postembryonic origin from the pericycle cell layer of the PR (Malamy and Benfey, 1997). Other differences in growth have been described; however, the mechanistic basis controlling such distinctions is unclear. The response to gravity, for example, differs between the PR and LR (Kiss et al., 2002; Guyomarc'h et al., 2012). The PR is able to immediately respond to the gravity vector and, in flax, is responsive even before germination (Ma and Hasenstein, 2006). On the other hand, newly emerged LRs in *Arabidopsis* show little sign of gravitropism initially and become more gravitropic over time. These differences have important effects on root system architecture and enable larger domains of the soil environment to be explored. Work by Guyomarc'h et al. revealed that the expression pattern of PIN transporters changes extensively through postemergence LR development, which suggests a potential mechanism to control the observed differences in gravitropism (Guyomarc'h et al., 2012).

In our study, we show that hormone and salt stress signaling differ significantly between LRs and PRs. Salt stress activates high levels of ABA signaling exclusively in LRs, as demonstrated by the LR-specific expression of the *ProRAB18*:*GFP* reporter. These data suggest that ABA signaling may have little activity in the PR at the concentrations of salt used here (100 mM NaCl). Indeed, all mutants affecting ABA signaling primarily rescue growth of the LR, while the PR is unaffected or grows slower. These data suggest that salt may induce LR-specific ABA biosynthesis or that the LR may be hypersensitive to ABA. Exogenous application of ABA clearly shows that the LR exhibits significantly higher sensitivity to ABA than the PR. Thus, we propose that LRs and PRs diverge in their salt response due to differences downstream of ABA biosynthesis. Root type–specific

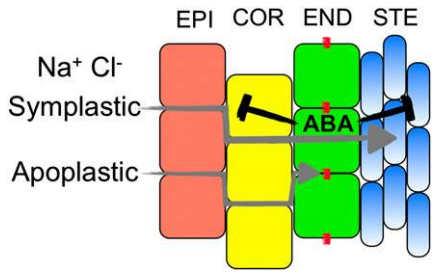

Figure 8. Model for the Regulation of LR Growth by NaCl-Triggered ABA Signaling.

Possible routes for the diffusion of NaCl associated ions through the tissues of the root are shown. Apoplastic movement of solutes can occur through the epidermis (EPI) and cortex (COR) but is blocked at the Casparian strip (red dashes) of the endodermis (END). Solutes entering into the stele (STE), where the vasculature is housed, must be transported into the symplast and pass through the cytoplasm of the endodermis. Sensing of sodium ions in the endodermal cytoplasm presumably triggers ABA signaling, which causes growth arrest of the neighboring tissues.
[See online article for color version of this figure.]

expression of the various components of the core ABA signaling pathway may be involved; however, no exhaustive profiling experiments have yet compared the transcriptomes of post-emergence LRs with PRs to uncover such differences.

In the shoot, well-characterized sets of transcription factors determine the identities of different meristem types (Bowman et al., 1993; Wellmer and Riechmann, 2010). The vegetative meristem of *Arabidopsis* transitions to an inflorescence meristem, and lateral branch meristems are specified as floral meristems. While currently uncharacterized, the various meristem types in the shoot may also have unique hormone and stress signaling properties that allow the plant to regulate context appropriate environmental responses. We speculate that post-emergent LRs may have a unique identity, in the developmental sense, that specifies the suite of genes controlling hormone, stress signaling, and gravity response. In species such as maize (*Zea mays*), where additional root types like seminal, crown, and brace roots occur, mechanisms to determine the identity of each root type may exist (Hochholdinger and Tuberosa, 2009). To understand how plants tailor stress signaling for particular environmental and field conditions, it will be important to understand the mechanisms that regulate the identity of each root type and the associated stress signaling networks.

Tissue-Specific ABA Signaling Regulates Root Growth

In our study, we examined the function of tissue-specific ABA signaling in the context of exogenous ABA treatment as well as an environmental stress that acts through the ABA pathway to regulate growth. These studies focused on LR growth but also examined the PR. This comparative approach enabled us to distinguish where ABA is able to regulate growth from where ABA actually acts during a physiologically relevant execution of the pathway. Interestingly, we find that the endodermis is not the only cell type where ABA signaling can regulate growth. With exogenous ABA treatment, the stele is also important. In other cell types, ABA signaling may control the same downstream pathways to affect growth. Alternatively, ABA signaling may regulate growth by distinct developmental mechanisms in each cell type. We find that the salt-induced expression of some ABA-regulated genes (e.g., *RD29A* and *ABI2*) is not strictly dependent on endodermal ABA signaling (Figure 5E). Consistent with these results, cell type–specific analysis shows that such genes are induced by salt stress in all root tissue layers (see Supplemental Figure 9A online). Thus, we propose that ABA signaling may be active in multiple tissue layers of the root during salt stress but that certain functions, such as growth regulation, are controlled by tissue-specific ABA signaling pathways.

Several recent studies have also highlighted the role of developmental pathways in the control of stress response. Iyer-Pascuzzi et al. (2011) have shown that the *scr* mutant, which disrupts the asymmetric division of the cortex/endodermal stem cell, has defects in germination upon ABA treatment (Cui et al., 2012). This work and another study by Cui et al. (2012) have shown that SCR can directly regulate the expression of several transcription factors controlling ABA response, including *HB12*, which we find here to be regulated by ABA signaling in the endodermis. Work presented here, along with these other studies, have now clearly demonstrated that developmental regulation and tissue-specific signaling are important for generating a stress response program and for salt tolerance (Møller et al., 2009), a model we proposed in our original work studying tissue-specific responses to abiotic stress (Dinneny et al., 2008).

The Endodermis as a Gateway with an ABA-Dependent Guard

The endodermis is an evolutionarily conserved cell type found in all flowering plants and acts as a semipermeable barrier due to the presence of a specialized cell wall modification termed the Casparian strip. Recent work has shown that lignin deposition in the Casparian strip primarily contributes to its function as a barrier to the apoplastic diffusion of solutes into the vascular stream (Roppolo et al., 2011; Naseer et al., 2012). Consequently, transport of solutes must occur by entering the symplast of the outer tissue layers or the endodermis itself. Thus, this cell type can be considered a gateway for entry into the vascular stream. Indeed, several transporters are expressed in this tissue layer and are localized to a specific side of the cell, consistent with their function in nutrient uptake (Ma et al., 2006, 2007; Alassimone et al., 2010; Takano et al., 2010; Sasaki et al., 2012).

For salinity stress, in particular, the extent to which a plant absorbs sodium into the vascular stream and transports it to the shoot is negatively correlated with overall stress tolerance (Munns, 2002; Møller and Tester, 2007). The endodermis may cause a bottleneck in the diffusion of sodium ions through the root, and as a consequence, ABA signaling may be most strongly activated there and growth arrested. This hypothesis is consistent with data from Møller et al. (2009) showing that, after salt treatment, sodium ions accumulate in the outer tissue layers of the root while the inner stele has lower levels. Use of a Casparian strip marker, *CASPARIAN STRIP MEMBRANE DOMAIN PROTEIN 1*:*GFP* (Roppolo et al., 2011), confirms that quiescent stage LRs form a well-developed Casparian strip under salt stress, while under standard conditions, LRs show less marker expression (see Supplemental Figure 13 online). These data are consistent with previous findings showing that salt can induce thickening of the Casparian strip in maize (Karahara et al., 2004). Endodermal cells may also be particularly sensitive to the presence of sodium ions and activate ABA signaling at a lower threshold than other cell types. As a consequence of either mechanism, ABA signaling would act as a guard at the endodermal gate, ensuring that growth of the LR does not proceed into high saline environments (Figure 8). The quiescent phase of growth induced by ABA appears to be necessary for acclimation and ultimate growth recovery, as plants suppressed in endodermal ABA signaling exhibit unsustainable growth. Thus, other processes besides growth regulation, such as the control of ion homeostasis, may be downstream of endodermal ABA signaling and enable long-term growth and acclimation.

METHODS

Plant Materials

Arabidopsis thaliana ecotypes Col-0, Landsberg *erecta* (L*er*), and Wassilewskija (Ws) were used in this study. The *abi1-1* (Armstrong et al., 1995), *abi2-1* (Leung et al., 1997), *abi3-1* (Nambara et al., 1995), *della quadruple*

mutants (Tyler et al., 2004), and the *ProRGA*:*GFP*:*RGA* (Achard et al., 2006) and *ProSCR*:*gai-1*:*GR* (Ubeda-Tomás et al., 2008) transgenes are in the L*er* background. The *abi4-1* (Finkelstein et al., 1998), *aba2-1* (Léon-Kloosterziel et al., 1996), *aba2-sail* (SAIL_407_E12), *nced2* (Toh et al., 2008), *nced3* (Ruggiero et al., 2004), *nced5* (Toh et al., 2008), *nced9* (Toh et al., 2008), *fus3-3* (Keith et al., 1994), *era1-1* (Cutler et al., 1996), *ein2-44* (Ghassemian et al., 2000), *ein3 eil1* (An et al., 2010), *lax3* (Swarup et al., 2008), *UAS*:*abi1-1*, *ProRAB18*:*GFP* (Kim et al., 2011), *CYCB1;1*:*GUS* (Colón-Carmona et al., 1999), *ProSHR*:*SHR*:*GR*, *shr-2*, *ProSCR*:*erGFP* (Levesque et al., 2006), and *CASP1*:*GFP* (Roppolo et al., 2011) transgenes are in the Col-0 background. The *abi5-1* (Finkelstein, 1994) mutation is in the Ws background. *GAL4-VP16*/*UAS* enhancer trap lines *J3411*, *J0951*, *J2812*, *J0571*, *Q2500*, *Q0990*, and *J0121* (Kiegle et al., 2000; Ubeda-Tomás et al., 2008) are in the C24 background.

Plant Growth Conditions

Seeds were surface sterilized by washing in a 95% ethanol solution for 5 min followed by a 5-min wash in a 20% bleach/0.1% Tween 20 solution. Seeds were then rinsed in sterile deionized water four times and stored in water for 2 d at 4°C. Sterilized seeds were grown on sterile 1% agar media containing 1× MS nutrients (MSP01-50LT; Caisson), 1% Suc, and 0.5 g/L MES, adjusted to pH 5.7 with KOH (termed "standard media"). Seedlings were grown for 6 d before transfer to standard media supplemented with NaCl or other chemicals for 3 to 7 d. Supplements include NaCl (Sigma-Aldrich), ABA (Sigma-Aldrich), ACC (Sigma-Aldrich), GA (Sigma-Aldrich), PAC (Sigma-Aldrich), and DEX (Sigma-Aldrich). The position of the root tip was marked at the time of transfer to distinguish the two regions of the root, A and B. Growth of seedlings was performed in a Percival CU41L4 incubator at a constant temperature of 22°C with long-day lighting conditions (16 h light and 8 h dark). Plates were partly sealed with Parafilm (Alcan Packaging) on three sides, while the top of the plate was sealed with micropore tape (3M) to allow for gas exchange. This was important for allowing a sufficient number of LRs to grow for observation.

Transgene Construction

The *UAS*:*abi1-1* construct was generated by mobilizing the *abi1-1* cDNA (with N-terminal triple myc tag) in plasmid pDONR207 (gift from J. Leung) into the plasmid pUAS-KWG (Karimi et al., 2002) between the UAS and NOS terminator sequences using a Gateway (Invitrogen) cloning approach. Transgenic plants were generated by a standard floral dip method (Clough and Bent, 1998).

To generate the *ProSCR*:*abi1-1*:*RFP* and *ProCOR*:*abi1-1*:*RFP* constructs, the primers 5′-caccATGGAGGAAGTATCTCCGGCG-3′ and 5′-GTTCAAGGGTTTGCTCTTGAG-3′ were used to PCR amplify the mutated *abi1-1* coding sequence without its stop codon from cDNA synthesized using *abi1-1* inflorescence RNA and cloned into the Gateway-compatible D-TOPO vector. Multisite Gateway (Invitrogen) recombination was used to introduce *ProSCR*:*abi1-1*:*RFP* and *ProCOR*:*abi1-1*:*RFP* into a dpGreen-based binary vector, which contains a kanamycin-resistant gene for plant selection.

To generate the *ProSCR*:*abi1-1* construct, the primers 5′-caccATGGAGGAAGTATCTCCGGCG-3′ and 5′-TCAGTTCAAGGGTTTGCTCTTG-3′ were used to PCR amplify the mutated *abi1-1* coding sequence. Multisite Gateway (Invitrogen) recombination (Karimi et al., 2005) was use to introduce a *ProSCR*:*abi1-1* minigene into a modified dpGreen-based binary vector, which contained a 35S:PM-mCherry selection marker in place of the kanamycin resistance gene (pCherry-pickerT).

Transgenic plants were generated using a modified floral dip method as follows. GV3101 cells were cultured in large Petri dishes (150-mm diameter) on selective Luria-Bertani agar media for 2 d at 28°C. Fifty milliliters of infiltration media (half-strength MS salts, 0.03% Silwet L77, and 5% Suc adjusted to pH 5.7 with KOH) was poured on top of the Luria-Bertani agar media and cells were scraped off into the solution. The cell suspension was homogenized by gentle shaking for 5 s in a 50-mL conical tube. The cell suspension was then diluted with an additional 150 mL of infiltration media and the combined solution used for floral dip–mediated plant transformation. Seeds were harvested from treated plants and selected visually based on mCherry fluorescence using an M165 FC fluorescence microscope (Leica).

Microscopy Analysis

For quantitation of LR developmental stages, roots were mounted in a modified Hoyer's solution (chloral hydrate:water:glycerol in proportions 8:2:1, g/mL/mL) and then imaged using a Leica DMI6000 inverted compound microscope. The GUS staining protocol was performed as previously described (Swarup et al., 2008). For confocal microscope imaging, roots were mounted in an FM4-64 solution (Invitrogen; Levesque et al., 2006) or propidium iodide (Invitrogen) and imaged using a Leica SP5 point-scanning confocal microscope. The imaging settings were 488-nm excitation and 505- to 550-nm emission for GFP and 488-nm excitation and >585-nm emission for FM4-64 or propidium iodide.

Phenotypic Analysis

For end-point analysis of root length, seedlings were grown on standard media for 6 d and then transferred to various conditions for 4 d. Images of 10 dpg seedlings were captured using a CanonScan 9000F flatbed scanner (Canon). The length of all visible LRs in root region A and PR length of region B was quantified using ImageJ (Abramoff et al., 2004). The average LR length and standard error of the mean per treatment were calculated from the average LR length of each seedling. Sample size of the various experiments is indicated in the corresponding figure legends.

For live-imaging analysis of LR growth, a custom live-imaging system was developed and consisted of the following: Samples were manipulated using a circular platform with six tissue-culture plate holders and controlled by an automated Theta/360 degree rotary stage and MFC-2000 controller (Applied Scientific Instrumentation), samples were backlit using an infrared light-emitting diode panel, and images were captured using a digital monochrome camera (CoolSnap) fitted with an NF Micro-Nikor 60-mm lens (Nikon) and infrared filter. Micro-Manager Software (Vale Lab, University of California, San Francisco) was used to control the stage and automate image acquisition (Edelstein et al., 2010). Images were taken every 15 min (wild-type growth under standard or salt stress conditions) or 20 min (transactivation of *abi1-1* studies) for 7 d. Sequential images were collated as a stack for further analysis using ImageJ. The StackReg plug-in was used to align the stack of image slices before root growth quantitation. Quantification of data from the time-lapse movies was conducted using the Manual Tracking plug-in for ImageJ. The growth of the root tip was tracked manually from frame to frame. Growth rate data were imported into TM4 microarray software suite (www.tm4.org/mev/) to generate heat maps (Saeed et al., 2006). Hierarchical clustering using Pearson correlation as the distance metric was performed to organize the growth data.

To determine the effect of salt stress on cell cycle activity in LRs, the expression of the *CYCLINB1;1*:*GUS* reporter was quantified in seedlings transferred to standard or 100 mM NaCl conditions for 3 d. The total number of GUS-positive and GUS-negative LRs was counted for LRs where obvious elongation and maturation zones had developed (long LRs) or where no such zonation had developed (short LRs).

To monitor dynamic changes in ABA signaling in LRs, fluorescence of the *ProRAB18*:*GFP* reporter was imaged on a Leica fluorescence dissecting microscope once per day of treatment. LR length and GFP fluorescence intensity at each time point was quantified using ImageJ (Abramoff et al., 2004). GFP was quantified by calculating the average

pixel intensity over the area of the entire LR. To monitor GFP:RGA accumulation, we quantified the average fluorescence intensity of nuclei in the endodermis using ImageJ.

Two-way analysis of variance and Student's *t* test were used to test for statistical significance in root length measurements using a P value threshold of <0.05 and a Bonferroni correction based on the number of tests performed.

Gene Expression

For qRT-PCR analysis of gene expression, RNA was extracted from root region A or region B separately using the RNeasy plant mini kit (Qiagen) according to manufacturer's instructions. cDNA was prepared using the iScript advanced cDNA synthesis kit (Bio-Rad) from 300 ng of total RNA. qRT-PCR was performed on a Fluidigm BioMark 96.96 Expression Chip using EvaGreen (Bio-Rad) as the fluorescence probe according to the Fluidigm Advanced Development Protocol #37. *AT3G07480* was used as a control gene because of its stable expression under various stresses (see Supplemental Figure 14 online). Two biological replicates and three technical replicates were used in this analysis. Technical replicates were averaged first, then average expression values were calculated from the biological replicates and imported into TM4 microarray software suite (www.tm4.org/index.html) to generate expression heat maps (Saeed et al., 2006). Expression values were unlog-transformed assuming two-fold amplification efficiency with each PCR cycle and normalized. Hierarchical clustering using Pearson correlation as the distance metric was performed to organize the expression data. Primers used in these experiments are listed in Supplemental Table 1 online.

Genetic Analysis

To selectively express *abi1-1* in different tissue types, various enhancer trap lines were crossed to plants harboring the *UAS:abi1-1* transgene. Wild-type plants of the C24 ecotype were crossed with *UAS:abi1-1* plants to generate the control genotype. Phenotypic and gene expression analysis were performed using the F1 seeds. To evaluate whether salt-dependent changes in RGA protein stability were ABA signaling dependent, *ProRGA:GFP:RGA* transgenic plants were crossed with the *abi1-1* mutant or to the L*er* ecotype to generate the control genotype. F1 seeds from these crosses were used for confocal image analysis of GFP:RGA fluorescence under standard or salt stress conditions.

Accession Numbers

Sequence data from this article can be found in the Arabidopsis Genome Initiative or GenBank/EMBL databases under accession number At4g26080 (*ABI1*). Gene IDs for genes used for real-time quantitative PCR can be found in Supplemental Table 1 online.

Supplemental Data

The following materials are available in the online version of this article.

Supplemental Figure 1. LR Growth Is More Strongly Suppressed Than PR Growth by Salt among Different Ecotypes.

Supplemental Figure 2. Quiescent LRs Have Normal Tissue Organization.

Supplemental Figure 3. ABA and ACC Treatments Show Different Trends in Their Effects on LR and PR Growth and Are Ecotype Independent.

Supplemental Figure 4. ABA Signaling Primarily Affects LR Growth under Salt Stress Conditions.

Supplemental Figure 5. Six Enhancer-Trap Lines Show Distinct Expression Patterns in *Arabidopsis* PRs.

Supplemental Figure 6. ABA Signaling in the Pericycle Does Not Significantly Regulate LR Growth during Salt Stress.

Supplemental Figure 7. Sucrose in the Media Does Not Affect the Salt Response of LRs in Control or *Q2500>>abi1-1* Transactivation Genotypes.

Supplemental Figure 8. Endodermis-Specific Expression of *abi1-1* Partially Rescues LR Growth during ABA and Salt Treatment.

Supplemental Figure 9. NaCl Regulates the Expression of ABA-Responsive Genes and Activates Prolonged Expression of the *ProRAB18:GFP* Reporter.

Supplemental Figure 10. Nutrient Conditions Modulate the Response of LRs and PRs to Salt Stress.

Supplemental Figure 11. The Salt Response of PRs Is Moderately Affected by Exogenous GA Treatment and by Endogenous GA Signaling.

Supplemental Figure 12. Interactions between ABA and GA Signaling and the Effect of DELLA Activity on LR Growth and Gene Expression.

Supplemental Figure 13. *ProCASP1:GFP* Expression Is Induced at an Earlier LR Stage and Is More Intensely Expressed under Salt Stress Conditions.

Supplemental Figure 14. *AT3G07480* Serves as the Control Gene for qRT-PCR Expression Assays in This Work Due to Its Stable Expression under Various Abiotic Stress Conditions.

Supplemental Table 1. Primer Sequences Used for Real-Time qPCR Experiments.

Supplemental Movie 1. Time-Lapse Movie of Col-0 Lateral Root Growth.

Supplemental Movie 2. Time-Lapse Movie of Lateral Root Growth in Control and *Q2500>>abi1-1* Transactivation Line under 100 mM NaCl.

ACKNOWLEDGMENTS

We thank Adrienne H.K. Roeder and members of the Dinneny lab for careful review of the article and Xueliang Wei for computational support. We thank Larry Cheung and microLambda Pte. Ltd. as well as Graham Wright for assistance designing and building the seedling live-imaging system used here. Funding of the portion of this work performed at the Temasek Lifesciences Laboratory was provided by the Singapore National Research Foundation. Research performed at the Carnegie Institution for Science was supported by the Carnegie Institution of Washington Endowment fund.

AUTHOR CONTRIBUTIONS

L.D. and J.R.D. designed the research plan. L.D. performed most of the experiments and data analysis. M.J.B., D.D., and R.B. originated the concept for inhibiting ABA signaling using *abi1-1* misexpression and generated the *UAS:abi1-1* transgenic line. C.H.N. generated the pCherry-pickerT vector. P.M.Y.C. established protocols for live imaging, image analysis, and high-throughput qRT-PCR. L.D. and J.R.D. wrote this article, which was read by all the authors.

Received November 6, 2012; revised December 19, 2012; accepted December 30, 2012; published January 22, 2013.

REFERENCES

Abramoff, M.D., Magelhaes, P.J., and Ram, S.J. (2004). Image processing with ImageJ. Biophotonics International **11:** 36–42.

Achard, P., Cheng, H., De Grauwe, L., Decat, J., Schoutteten, H., Moritz, T., Van Der Straeten, D., Peng, J., and Harberd, N.P. (2006). Integration of plant responses to environmentally activated phytohormonal signals. Science **311:** 91–94.

Alassimone, J., Naseer, S., and Geldner, N. (2010). A developmental framework for endodermal differentiation and polarity. Proc. Natl. Acad. Sci. USA **107:** 5214–5219.

An, F., et al. (2010). Ethylene-induced stabilization of *ETHYLENE INSENSITIVE3* and *EIN3-LIKE1* is mediated by proteasomal degradation of *EIN3* binding F-box 1 and 2 that requires *EIN2* in *Arabidopsis*. Plant Cell **22:** 2384–2401.

Armstrong, F., Leung, J., Grabov, A., Brearley, J., Giraudat, J., and Blatt, M.R. (1995). Sensitivity to abscisic acid of guard-cell K^+ channels is suppressed by *abi1-1*, a mutant *Arabidopsis* gene encoding a putative protein phosphatase. Proc. Natl. Acad. Sci. USA **92:** 9520–9524.

Benková, E., Michniewicz, M., Sauer, M., Teichmann, T., Seifertová, D., Jürgens, G., and Friml, J. (2003). Local, efflux-dependent auxin gradients as a common module for plant organ formation. Cell **115:** 591–602.

Bowman, J.L., Alvarez, J., Weigel, D., Meyerowitz, E.M., and Smyth, D.R. (1993). Control of flower development in *Arabidopsis thaliana* by *APETALA1* and interacting genes. Development **119:** 721–743.

Burssens, S., Himanen, K., van de Cotte, B., Beeckman, T., Van Montagu, M., Inzé, D., and Verbruggen, N. (2000). Expression of cell cycle regulatory genes and morphological alterations in response to salt stress in *Arabidopsis thaliana*. Planta **211:** 632–640.

Clough, S.J., and Bent, A.F. (1998). Floral dip: A simplified method for *Agrobacterium*-mediated transformation of *Arabidopsis thaliana*. Plant J. **16:** 735–743.

Colón-Carmona, A., You, R., Haimovitch-Gal, T., and Doerner, P. (1999). Technical advance: Spatio-temporal analysis of mitotic activity with a labile cyclin-GUS fusion protein. Plant J. **20:** 503–508.

Cui, H., Hao, Y., and Kong, D. (2012). *SCARECROW* has a *SHORT-ROOT*-independent role in modulating the sugar response. Plant Physiol. **158:** 1769–1778.

Cui, H., Levesque, M.P., Vernoux, T., Jung, J.W., Paquette, A.J., Gallagher, K.L., Wang, J.Y., Blilou, I., Scheres, B., and Benfey, P.N. (2007). An evolutionarily conserved mechanism delimiting *SHR* movement defines a single layer of endodermis in plants. Science **316:** 421–425.

Cutler, S., Ghassemian, M., Bonetta, D., Cooney, S., and McCourt, P. (1996). A protein farnesyl transferase involved in abscisic acid signal transduction in *Arabidopsis*. Science **273:** 1239–1241.

de Almeida Engler, J., De Vleesschauwer, V., Burssens, S., Celenza, J.L., Jr., Inzé, D., Van Montagu, M., Engler, G., and Gheysen, G. (1999). Molecular markers and cell cycle inhibitors show the importance of cell cycle progression in nematode-induced galls and syncytia. Plant Cell **11:** 793–808.

De Smet, I., Signora, L., Beeckman, T., Inzé, D., Foyer, C.H., and Zhang, H. (2003). An abscisic acid-sensitive checkpoint in lateral root development of *Arabidopsis*. Plant J. **33:** 543–555.

De Smet, I., et al. (2007). Auxin-dependent regulation of lateral root positioning in the basal meristem of *Arabidopsis*. Development **134:** 681–690.

Di Laurenzio, L., Wysocka-Diller, J., Malamy, J.E., Pysh, L., Helariutta, Y., Freshour, G., Hahn, M.G., Feldmann, K.A., and Benfey, P.N. (1996). The *SCARECROW* gene regulates an asymmetric cell division that is essential for generating the radial organization of the *Arabidopsis* root. Cell **86:** 423–433.

Dinneny, J.R. (2010). Analysis of the salt-stress response at cell-type resolution. Plant Cell Environ. **33:** 543–551.

Dinneny, J.R., Long, T.A., Wang, J.Y., Jung, J.W., Mace, D., Pointer, S., Barron, C., Brady, S.M., Schiefelbein, J., and Benfey, P.N. (2008). Cell identity mediates the response of *Arabidopsis* roots to abiotic stress. Science **320:** 942–945.

Dubrovsky, J.G., Sauer, M., Napsucialy-Mendivil, S., Ivanchenko, M.G., Friml, J., Shishkova, S., Celenza, J., and Benková, E. (2008). Auxin acts as a local morphogenetic trigger to specify lateral root founder cells. Proc. Natl. Acad. Sci. USA **105:** 8790–8794.

Edelstein, A., Amodaj, N., Hoover, K., Vale, R., and Stuurman, N. (2010). Computer control of microscopes using microManager. Curr. Protoc. Mol. Biol. **14:** 20.

Finkelstein, R., Reeves, W., Ariizumi, T., and Steber, C. (2008). Molecular aspects of seed dormancy. Annu. Rev. Plant Biol. **59:** 387–415.

Finkelstein, R.R. (1994). Mutations at two new *Arabidopsis* ABA response loci are similar to the *abi3* mutations. Plant J. **5:** 765–771.

Finkelstein, R.R., Wang, M.L., Lynch, T.J., Rao, S., and Goodman, H.M. (1998). The *Arabidopsis* abscisic acid response locus *ABI4* encodes an *APETALA 2* domain protein. Plant Cell **10:** 1043–1054.

Flowers, T.J., Garcia, A., Koyama, M., and Yeo, A.R. (1997). Breeding for salt tolerance in crop plants- The role of molecular biology. Acta Physiol. Plant. **19:** 427–433.

Fujii, H., Chinnusamy, V., Rodrigues, A., Rubio, S., Antoni, R., Park, S.Y., Cutler, S.R., Sheen, J., Rodriguez, P.L., and Zhu, J.K. (2009). In vitro reconstitution of an abscisic acid signalling pathway. Nature **462:** 660–664.

Ghassemian, M., Nambara, E., Cutler, S., Kawaide, H., Kamiya, Y., and McCourt, P. (2000). Regulation of abscisic acid signaling by the ethylene response pathway in *Arabidopsis*. Plant Cell **12:** 1117–1126.

Giehl, R.F.H., Lima, J.E., and von Wirén, N. (2012). Localized iron supply triggers lateral root elongation in *Arabidopsis* by altering the *AUX1*-mediated auxin distribution. Plant Cell **24:** 33–49.

Gifford, M.L., Dean, A., Gutierrez, R.A., Coruzzi, G.M., and Birnbaum, K.D. (2008). Cell-specific nitrogen responses mediate developmental plasticity. Proc. Natl. Acad. Sci. USA **105:** 803–808.

González-García, M.P., Vilarrasa-Blasi, J., Zhiponova, M., Divol, F., Mora-García, S., Russinova, E., and Caño-Delgado, A.I. (2011). Brassinosteroids control meristem size by promoting cell cycle progression in *Arabidopsis* roots. Development **138:** 849–859.

Guyomarc'h, S., Léran, S., Auzon-Cape, M., Perrine-Walker, F., Lucas, M., and Laplaze, L. (2012). Early development and gravitropic response of lateral roots in *Arabidopsis thaliana*. Philos. Trans. R. Soc. Lond. B Biol. Sci. **367:** 1509–1516.

Hacham, Y., Holland, N., Butterfield, C., Úbeda-Tomás, S., Bennett, M.J., Chory, J., and Savaldi-Goldstein, S. (2011). Brassinosteroid perception in the epidermis controls root meristem size. Development **138:** 839–848.

Harberd, N.P., Belfield, E., and Yasumura, Y. (2009). The angiosperm gibberellin-GID1-DELLA growth regulatory mechanism: How an "inhibitor of an inhibitor" enables flexible response to fluctuating environments. Plant Cell **21:** 1328–1339.

He, X.J., Mu, R.L., Cao, W.H., Zhang, Z.G., Zhang, J.S., and Chen, S.Y. (2005). *AtNAC2*, a transcription factor downstream of ethylene and auxin signaling pathways, is involved in salt stress response and lateral root development. Plant J. **44:** 903–916.

Helariutta, Y., Fukaki, H., Wysocka-Diller, J., Nakajima, K., Jung, J., Sena, G., Hauser, M.T., and Benfey, P.N. (2000). The *SHORT-ROOT* gene controls radial patterning of the *Arabidopsis* root through radial signaling. Cell **101:** 555–567.

Hochholdinger, F., and Tuberosa, R. (2009). Genetic and genomic dissection of maize root development and architecture. Curr. Opin. Plant Biol. **12:** 172–177.

Hubbard, K.E., Nishimura, N., Hitomi, K., Getzoff, E.D., and Schroeder, J.I. (2010). Early abscisic acid signal transduction mechanisms: Newly discovered components and newly emerging questions. Genes Dev. **24:** 1695–1708.

Iyer-Pascuzzi, A.S., Jackson, T., Cui, H., Petricka, J.J., Busch, W., Tsukagoshi, H., and Benfey, P.N. (2011). Cell identity regulators link development and stress responses in the *Arabidopsis* root. Dev. Cell **21:** 770–782.

Karahara, I., Ikeda, A., Kondo, T., and Uetake, Y. (2004). Development of the Casparian strip in primary roots of maize under salt stress. Planta **219:** 41–47.

Karimi, M., De Meyer, B., and Hilson, P. (2005). Modular cloning in plant cells. Trends Plant Sci. **10:** 103–105.

Karimi, M., Inzé, D., and Depicker, A. (2002). GATEWAY vectors for *Agrobacterium*-mediated plant transformation. Trends Plant Sci. **7:** 193–195.

Keith, K., Kraml, M., Dengler, N.G., and McCourt, P. (1994). *fusca3*: A heterochronic mutation affecting late embryo development in *Arabidopsis*. Plant Cell **6:** 589–600.

Kiegle, E., Moore, C.A., Haseloff, J., Tester, M.A., and Knight, M.R. (2000). Cell-type-specific calcium responses to drought, salt and cold in the *Arabidopsis* root. Plant J. **23:** 267–278.

Kim, T.H., et al. (2011). Chemical genetics reveals negative regulation of abscisic acid signaling by a plant immune response pathway. Curr. Biol. **21:** 990–997.

Kiss, J.Z., Miller, K.M., Ogden, L.A., and Roth, K.K. (2002). Phototropism and gravitropism in lateral roots of *Arabidopsis*. Plant Cell Physiol. **43:** 35–43.

Laskowski, M., Grieneisen, V.A., Hofhuis, H., Hove, C.A., Hogeweg, P., Marée, A.F., and Scheres, B. (2008). Root system architecture from coupling cell shape to auxin transport. PLoS Biol. **6:** e307.

Lee, J.Y., Colinas, J., Wang, J.Y., Mace, D., Ohler, U., and Benfey, P.N. (2006). Transcriptional and posttranscriptional regulation of transcription factor expression in *Arabidopsis* roots. Proc. Natl. Acad. Sci. USA **103:** 6055–6060.

Léon-Kloosterziel, K.M., Gil, M.A., Ruijs, G.J., Jacobsen, S.E., Olszewski, N.E., Schwartz, S.H., Zeevaart, J.A.D., and Koornneef, M. (1996). Isolation and characterization of abscisic acid-deficient *Arabidopsis* mutants at two new loci. Plant J. **10:** 655–661.

Leung, J., Merlot, S., and Giraudat, J. (1997). The *Arabidopsis ABSCISIC ACID-INSENSITIVE2* (*ABI2*) and *ABI1* genes encode homologous protein phosphatases 2C involved in abscisic acid signal transduction. Plant Cell **9:** 759–771.

Levesque, M.P., Vernoux, T., Busch, W., Cui, H., Wang, J.Y., Blilou, I., Hassan, H., Nakajima, K., Matsumoto, N., Lohmann, J.U., Scheres, B., and Benfey, P.N. (2006). Whole-genome analysis of the *SHORT-ROOT* developmental pathway in *Arabidopsis*. PLoS Biol. **4:** e143.

Linkohr, B.I., Williamson, L.C., Fitter, A.H., and Leyser, H.M. (2002). Nitrate and phosphate availability and distribution have different effects on root system architecture of *Arabidopsis*. Plant J. **29:** 751–760.

Little, D.Y., Rao, H., Oliva, S., Daniel-Vedele, F., Krapp, A., and Malamy, J.E. (2005). The putative high-affinity nitrate transporter NRT2.1 represses lateral root initiation in response to nutritional cues. Proc. Natl. Acad. Sci. USA **102:** 13693–13698.

López-Bucio, J., Cruz-Ramírez, A., and Herrera-Estrella, L. (2003). The role of nutrient availability in regulating root architecture. Curr. Opin. Plant Biol. **6:** 280–287.

Lucas, M., et al. (2011). *Short-Root* regulates primary, lateral, and adventitious root development in *Arabidopsis*. Plant Physiol. **155:** 384–398.

Ma, J.F., Tamai, K., Yamaji, N., Mitani, N., Konishi, S., Katsuhara, M., Ishiguro, M., Murata, Y., and Yano, M. (2006). A silicon transporter in rice. Nature **440:** 688–691.

Ma, J.F., Yamaji, N., Mitani, N., Tamai, K., Konishi, S., Fujiwara, T., Katsuhara, M., and Yano, M. (2007). An efflux transporter of silicon in rice. Nature **448:** 209–212.

Ma, Y., Szostkiewicz, I., Korte, A., Moes, D., Yang, Y., Christmann, A., and Grill, E. (2009). Regulators of PP2C phosphatase activity function as abscisic acid sensors. Science **324:** 1064–1068.

Ma, Z., and Hasenstein, K.H. (2006). The onset of gravisensitivity in the embryonic root of flax. Plant Physiol. **140:** 159–166.

Malamy, J.E. (2005). Intrinsic and environmental response pathways that regulate root system architecture. Plant Cell Environ. **28:** 67–77.

Malamy, J.E., and Benfey, P.N. (1997). Organization and cell differentiation in lateral roots of *Arabidopsis thaliana*. Development **124:** 33–44.

Meyer, K., Leube, M.P., and Grill, E. (1994). A protein phosphatase 2C involved in ABA signal transduction in *Arabidopsis thaliana*. Science **264:** 1452–1455.

Møller, I.S., Gilliham, M., Jha, D., Mayo, G.M., Roy, S.J., Coates, J.C., Haseloff, J., and Tester, M. (2009). Shoot Na^+ exclusion and increased salinity tolerance engineered by cell type-specific alteration of Na^+ transport in *Arabidopsis*. Plant Cell **21:** 2163–2178.

Møller, I.S., and Tester, M. (2007). Salinity tolerance of *Arabidopsis*: A good model for cereals? Trends Plant Sci. **12:** 534–540.

Moreno-Risueno, M.A., Van Norman, J.M., Moreno, A., Zhang, J., Ahnert, S.E., and Benfey, P.N. (2010). Oscillating gene expression determines competence for periodic *Arabidopsis* root branching. Science **329:** 1306–1311.

Munns, R. (2002). Comparative physiology of salt and water stress. Plant Cell Environ. **25:** 239–250.

Mustroph, A., Zanetti, M.E., Jang, C.J., Holtan, H.E., Repetti, P.P., Galbraith, D.W., Girke, T., and Bailey-Serres, J. (2009). Profiling translatomes of discrete cell populations resolves altered cellular priorities during hypoxia in *Arabidopsis*. Proc. Natl. Acad. Sci. USA **106(44):** 18843–18848.

Nambara, E., McCourt, P., and Naito, S. (1995). A regulatory role for the *ABI3* gene in the establishment of embryo maturation in *Arabidopsis thaliana*. Development **121:** 629–636.

Naseer, S., Lee, Y., Lapierre, C., Franke, R., Nawrath, C., and Geldner, N. (2012). Casparian strip diffusion barrier in *Arabidopsis* is made of a lignin polymer without suberin. Proc. Natl. Acad. Sci. USA **109:** 10101–10106.

Okushima, Y., Inamoto, H., and Umeda, M. (2011). A high concentration of nitrate causes temporal inhibition of lateral root growth by suppressing cell proliferation. Plant Biotechnol. **28:** 413–416.

Olsson, A.S., Engström, P., and Söderman, E. (2004). The homeobox genes *ATHB12* and *ATHB7* encode potential regulators of growth in response to water deficit in *Arabidopsis*. Plant Mol. Biol. **55:** 663–677.

Overvoorde, P., Fukaki, H., and Beeckman, T. (2010). Auxin control of root development. Cold Spring Harb. Perspect. Biol. **2:** a001537.

Park, S.Y., et al. (2009). Abscisic acid inhibits type 2C protein phosphatases via the PYR/PYL family of START proteins. Science **324:** 1068–1071.

Roppolo, D., De Rybel, B., Tendon, V.D., Pfister, A., Alassimone, J., Vermeer, J.E., Yamazaki, M., Stierhof, Y.D., Beeckman, T., and Geldner, N. (2011). A novel protein family mediates Casparian strip formation in the endodermis. Nature **473:** 380–383.

Ruggiero, B., Koiwa, H., Manabe, Y., Quist, T.M., Inan, G., Saccardo, F., Joly, R.J., Hasegawa, P.M., Bressan, R.A., and Maggio, A. (2004). Uncoupling the effects of abscisic acid on plant growth and water relations. Analysis of *sto1/nced3*, an abscisic acid-deficient but salt stress-tolerant mutant in *Arabidopsis*. Plant Physiol. **136:** 3134–3147.

Sasaki, A., Yamaji, N., Yokosho, K., and Ma, J.F. (2012). *Nramp5* is a major transporter responsible for manganese and cadmium uptake in rice. Plant Cell **24:** 2155–2167.

Savaldi-Goldstein, S., Peto, C., and Chory, J. (2007). The epidermis both drives and restricts plant shoot growth. Nature **446:** 199–202.

Saeed, A.I., Bhagabati, N.K., Braisted, J.C., Liang, W., Sharov, V., Howe, E.A., Li, J., Thiagarajan, M., White, J.A., and Quackenbush, J. (2006). TM4 microarray software suite. Methods Enzymol. **411:** 134–193.

Sharp, R.E., and LeNoble, M.E. (2002). ABA, ethylene and the control of shoot and root growth under water stress. J. Exp. Bot. **53:** 33–37.

Signora, L., De Smet, I., Foyer, C.H., and Zhang, H. (2001). ABA plays a central role in mediating the regulatory effects of nitrate on root branching in *Arabidopsis*. Plant J. **28:** 655–662.

Skirycz, A., and Inzé, D. (2010). More from less: Plant growth under limited water. Curr. Opin. Biotechnol. **21:** 197–203.

Son, O., et al. (2010). *ATHB12*, an ABA-inducible homeodomain-leucine zipper (HD-Zip) protein of *Arabidopsis*, negatively regulates the growth of the inflorescence stem by decreasing the expression of a gibberellin 20-oxidase gene. Plant Cell Physiol. **51:** 1537–1547.

Sozzani, R., Cui, H., Moreno-Risueno, M.A., Busch, W., Van Norman, J.M., Vernoux, T., Brady, S.M., Dewitte, W., Murray, J.A., and Benfey, P.N. (2010). Spatiotemporal regulation of cell-cycle genes by *SHORTROOT* links patterning and growth. Nature **466:** 128–132.

Spollen, W.G., LeNoble, M.E., Samuels, T.D., Bernstein, N., and Sharp, R.E. (2000). Abscisic acid accumulation maintains maize primary root elongation at low water potentials by restricting ethylene production. Plant Physiol. **122:** 967–976.

Swarup, K., et al. (2008). The auxin influx carrier *LAX3* promotes lateral root emergence. Nat. Cell Biol. **10:** 946–954.

Swarup, R., Kramer, E.M., Perry, P., Knox, K., Leyser, H.M., Haseloff, J., Beemster, G.T., Bhalerao, R., and Bennett, M.J. (2005). Root gravitropism requires lateral root cap and epidermal cells for transport and response to a mobile auxin signal. Nat. Cell Biol. **7:** 1057–1065.

Takano, J., Tanaka, M., Toyoda, A., Miwa, K., Kasai, K., Fuji, K., Onouchi, H., Naito, S., and Fujiwara, T. (2010). Polar localization and degradation of *Arabidopsis* boron transporters through distinct trafficking pathways. Proc. Natl. Acad. Sci. USA **107:** 5220–5225.

Toh, S., et al. (2008). High temperature-induced abscisic acid biosynthesis and its role in the inhibition of gibberellin action in *Arabidopsis* seeds. Plant Physiol. **146:** 1368–1385.

Tyler, L., Thomas, S.G., Hu, J., Dill, A., Alonso, J.M., Ecker, J.R., and Sun, T.P. (2004). Della proteins and gibberellin-regulated seed germination and floral development in *Arabidopsis*. Plant Physiol. **135:** 1008–1019.

Ubeda-Tomás, S., Federici, F., Casimiro, I., Beemster, G.T., Bhalerao, R., Swarup, R., Doerner, P., Haseloff, J., and Bennett, M.J. (2009). Gibberellin signaling in the endodermis controls *Arabidopsis* root meristem size. Curr. Biol. **19:** 1194–1199.

Úbeda-Tomás, S., Swarup, R., Coates, J., Swarup, K., Laplaze, L., Beemster, G.T.S., Hedden, P., Bhalerao, R., and Bennett, M.J. (2008). Root growth in *Arabidopsis* requires gibberellin/DELLA signalling in the endodermis. Nat. Cell Biol. **10:** 625–628.

Wee, C.W., and Dinneny, J.R. (2010). Tools for high-spatial and temporal-resolution analysis of environmental responses in plants. Biotechnol. Lett. **32:** 1361–1371.

Wellmer, F., and Riechmann, J.L. (2010). Gene networks controlling the initiation of flower development. Trends Genet. **26:** 519–527.

Winter, D., Vinegar, B., Nahal, H., Ammar, R., Wilson, G.V., and Provart, N.J. (2007). An "Electronic Fluorescent Pictograph" browser for exploring and analyzing large-scale biological data sets. PLoS ONE **2:** e718.

Zhang, H., and Forde, B.G. (1998). An *Arabidopsis* MADS box gene that controls nutrient-induced changes in root architecture. Science **279:** 407–409.

Zhu, J.K. (2002). Salt and drought stress signal transduction in plants. Annu. Rev. Plant Biol. **53:** 247–273.

Zhu, J.K., Liu, J., and Xiong, L. (1998). Genetic analysis of salt tolerance in *Arabidopsis*. Evidence for a critical role of potassium nutrition. Plant Cell **10:** 1181–1191.